

Selbstorganisierte molekulare Polygone aus konjugierten
1,1'-Ferrocendiyl-verbrückten Bis(pyridinen), Bis(2,2'-bipyridinen) und
Bis(1,10-phenanthrolinen) und Übergangsmetallen als Bausteine

**Molecular Polygons Self-Assembled from Conjugated
1,1'-Ferrocenediyl Bridged Bis(pyridines), Bis(2,2'-bipyridines), and
Bis(1,10-phenanthrolines) and Transition Metals as Building Blocks**

Dissertation

der Fakultät für Chemie und Pharmazie
der Eberhard-Karls-Universität Tübingen

zur Erlangung des Grades eines Doktors
der Naturwissenschaften

2002

vorgelegt von

Ruifa Zong

Tag der mündlichen Prüfung:

9. Oktober 2002

Dekan:

Prof. Dr. H. Probst

1. Berichterstatter:

Prof. Dr. E. Lindner

2. Berichterstatter:

Prof. Dr. Dr.h.c. J. Strähle

To my parents

To my wife and to our daughter

Die vorliegende Arbeit wurde am
Institut für Anorganische Chemie
der Eberhard-Karls-Universität
Tübingen unter der Leitung von
Herrn Prof. Dr. rer. nat.
Ekkehard Lindner angefertigt.

Meinem Doktorvater,
Herrn Prof. Dr. Ekkehard Lindner
danke ich sehr herzlich für die
Themenstellung, für die Bereit-
stellung ausgezeichneter Ar-
beitsbedingungen, die wertvollen
Anregungen und Diskussionen
sowie sein stetes Interesse an
dieser Arbeit

Ich möchte mich sehr herzlich bedanken bei:

Herrn Dr. Klaus Eichele, Herrn Manfred Steimann und Herrn Dr. Markus Ströbele für die Durchführung der Röntgenstrukturanalysen,

Frau Heike Dorn, Frau Angelika Ehmann und den Meßberechtigten am 250 MHz DRX-Gerät für Hochauflösungs-NMR-Messungen und nicht zu vergessen Herrn Dr. Ulf Kehrer, Herrn Dr. Jost Grimm und Herrn Prof. Dr. H. A. Mayer für zahlreiche Gespräche sowie deren stete Hilfsbereitschaft,

Frau Dr. Monika Förster, Herrn Dr. Joachim Wald und Herrn Dipl.-Chem. Michael Henes für die Beseitigung technischer Probleme,

Herrn Prof. Dr. B. Speiser für die Hilfe bei der Auswertung der cyclovoltammetrischen Messungen,

den Herren Bartholomä und Müller für die geduldige Durchführung zahlreicher Massenspektren, Herrn Wolfgang Bock für sein stetes Bemühen um gute Elementaranalysen,

Frau Barbara Saller für die Messung der IR-Spektren,

Frau Dipl. -Chem. Ulrike Weisser für die magnetischen Messungen, sowie Herrn Prof. Dr. H. -J. Meyer und Herrn Dr. Wolfgang Wischert für zahlreiche Gespräche,

Herrn Dr. Ilmari Krebs für die Unterstützung bei Literaturrecherchen,

Herrn Dr. Frank Höhn und Herrn Dr. Thomas Salesch für die Hilfe bei der Behebung von Computerproblemen,

Herrn Dr. Christoph Ayasse und Herrn Dr. Klaus Eichele für die zahlreiche Diskussionen,

Frau Roswitha Conrad und Herrn Dr. H.-D. Ebert für die unbürokratische Hilfe bei bürokratischen Problemen,

Herrn Dr. Christian Hermann, Herrn Dr. Markus Mohr, Herrn Dr. Robert Veigel, Herrn Dr. Markus Schmid, Herrn Dr. J. Wolfram Wielandt, Herrn Dr. Stefan Brugger, Herrn Dr. Monther Khanfar, Herrn Dr. Samer Al-Gharabli, Herrn Dr. Zhong-Lin Lu, Herrn Dipl.-Chem. Stephan Fuchs, Herrn M.S. Mahmoud Sunjuk, und Herrn M.S. Ismail Khalil Warad für die Anregungen und gute Kameradschaft,

Frau Elli Oster, Herrn Peter Wegner sowie allen technischen Angestellten, Praktikanten und Kollegen, die in irgendeiner Form zum Gelingen dieser Arbeit beigetragen haben.

Mein ganz besonderer Dank gilt meine Frau Yanjie Zhao und unsere Tochter Ying.

1	Introduction	1
2	General Section	3
2.1	Design of the Polydentate Ligands 1a-c and 10a-d	3
2.2	Bis(pyridine), Bis(bipyridine), and Bis(phenanthroline) Ligands 1a-c and 10a-d	3
2.2.1	Syntheses of Ligands 1a-c and 10a-d	3
2.2.2	NMR and IR Spectroscopic Characterization of 1a-c and 10a-d	9
2.2.3	Discussion of the Crystal Structures of 1a and 1b	13
2.3	Heterotetranuclear Molecular Polygons 11a,b and 12b	16
2.3.1	Syntheses of the Macrocycles 11a,b and 12b	16
2.3.2	¹ H NMR and IR Spectroscopic Characterization of the Macrocycles 11a,b and 12b	16
2.3.3	Discussion of the Crystal Structures of 11a,b and 12b	18
2.4	Binuclear Macrocycles 13c , 13d , 14d , and 15d	27
2.4.1	Syntheses and Properties of 13c , 13d , 14d , and 15d	27
2.4.2	¹ H NMR, MS, and IR Spectroscopic Characterization of 13c , 13d , 14d , and 15d	27
2.5	Electrochemical Investigations.....	29
2.6	Magnetic Investigation of Complex 11a	31
2.7	Conclusion.....	33
3	Experimental	35
3.1	General Considerations	35
3.1.1	Working Procedures	35

3.1.2	Charaterization.....	35
3.1.3	Starting Materials.....	35
3.2	Preparation of the Compounds.....	36
3.2.1	General Procedure for the Synthesis of 1a-c	36
3.2.1.1	1,1'-Bis(4-pyridylethynyl)ferrocene (1a).....	36
3.2.1.2	1,1'-Bis(3-pyridylethynyl)ferrocene (1b).....	36
3.2.1.3	1,1'-Bis(2,2'-bipyridine-5-ylethynyl)ferrocene (1c).....	37
3.2.2	1,1'-Bis{[2,5-dipropoxy-4-(triisopropylsilylethynyl)phenyl]ethynyl}- ferrocene (8).....	37
3.2.3	General Procedure for the Preparation of Ligands 10a-d	38
3.2.3.1	1,1'-Bis{[4-(4-pyridylethynyl)-2,5-dipropoxyphenyl]ethynyl}- ferrocene (10a).....	38
3.2.3.2	1,1'-Bis{[4-(3-pyridylethynyl)-2,5-dipropoxyphenyl]ethynyl}- ferrocene (10b).....	39
3.2.3.3	1,1'-Bis{[4-(2,2'-bipyridine-5-ylethynyl)-2,5-dipropoxy-phenyl]ethynyl}- ferrocene (10c).....	39
3.2.3.4	1,1'-Bis{[4-(1,10-phenanthroline-3-ylethynyl)-2,5-dipropoxy- phenyl]ethynyl}ferrocene (10d).....	40
3.2.4	Preparation of Macrocyclces 11a,b and 12b	41
3.2.4.1	Heterotetranuclear Fe ₂ Ni ₂ Complex 11a	41
3.2.4.2	Heterotetranuclear Fe ₂ Ag ₂ Complex 11b	41
3.2.4.3	Heterotetranuclear Fe ₂ Pd ₂ Complex 12b	42
3.2.5	General Procedure for the Preparation of the Bimetallic Complexes.....	42
3.2.5.1	Zn(CH ₃ COO) ₂ · 10c (13c).....	43
3.2.5.2	Zn(CH ₃ CO ₂) ₂ · 10d (13d).....	43

3.2.5.3	$\text{Ag}(\text{CF}_3\text{SO}_3) \cdot \mathbf{10d}$ (14d).....	43
3.2.5.4	$\text{Fe}(\text{ClO}_4)_2 \cdot \mathbf{10d}$ (15d)	44
3.3	X-ray Crystallographic Studies	44
3.4	Electrochemical Experiments	45
3.5	Magnetic Experiment	46
4	References	53
5	Summary	57

Abbreviations and Definitions

Å	Angström (10^{-10} m)
bipy	2,2'-Bipyridine
COD	1,5-Cyclooctadiene
Cp	Cyclopentadienyl
DMF	Dimethylformamide
DMSO	Dimethylsulfoxide
EI	Electron ionisation
FAB	Fast atom bombardment
FD	Field desorption
FT	Fourier transformation
g	Gram
h	Hour
Hz	Hertz
IR	Infrared spectroscopy
MHz	Megahertz
mg	Miligram
mL	Milliliter
mmol	Millimole
MS	Mass spectroscopy
nm	Nanometer
NMR	Nuclear magnetic resonance
phen	1,10-Phenanthroline
ppm	Parts per million
py	Pyridine
TBAF	Tetrabutylammonium fluoride
THF	Tetrahydrofuran
TIPSA	Triisopropylsilylacetylene
TMSA	Trimethylsilylacetylene
δ	Chemical shift

1 Introduction

Due to the potential application in material sciences as molecular devices and electronic sensors, the incorporation of redox active metallocenes in supramolecular structures encounters increasing interest in recent years.^[1-8] Systems of this type open the possibility to study electronic communication between metal based centers. Long distance electronic communication is an important topic for biology and molecular electronics.^[9-11] Basically, there is a distinction between two different effects, namely through bond and through space, or through solvents in solution. The former is more effective than the latter^[12] and the redox properties can be easily controlled.^[13,14] Several factors such as host/guest interactions,^[15] the nature of connectors between the metal centers,^[16-18] structural rearrangements,^[18,19] orbital alignments,^[20] orbital orderings,^[21] medium effects,^[22] and in particular the distance between the metals^[16,23] are influencing the degree of electronic communication. Therefore, it is important to construct molecules which guarantee to keep the metals well separated from each other to rule out through space electronic communication. Furthermore, it was demonstrated that the degree of conjugation within the molecular backbone between the transition metals also plays an important role.^[24,25]

On the other hand, a great number of bis(pyridine) functionalized ligands with different angles between their binding sites have been rationally designed, synthesized, and reacted with transition metal complexes to obtain two-dimensional macrocyclic molecular assemblies, such as molecular squares, triangles, and other polygons.^[26,27] With the increasing multitude of motifs self-assembled from these nitrogen functionalized building blocks, a library of such supramolecular architectures has been set up.^[28] Stang and Fujita made a lot of contributions to this field, however, they mainly employed pre-constructed *cis*-ML₂ (M = Pd/Pt) units.^[26-29] Both metals are electrochemically and magnetically inert. Hence, it is desirable to make accessible molecular polygons and polyhedra with magnetic and redox active centers.^[26,30] Although 1,1'-bis(diphenylphosphino)ferrocene (dppf) has been incorporated to get redox active molecular

squares, the *syn*-dppf conformer is not part of the backbones.^[26,31] A structurally characterized molecular square containing an *anti*-1,1'-ferrocenedicarboxylate moiety in its backbone was recently reported by Cotton et al.^[29,30] Compared to systems assembled via *non*-ferrocene bridges, its electrochemical property is described as peculiar. The preparation of self-assembled structures that contain functionalized sites, capable of showing interesting electronic, magnetic, and optical properties is still a big challenge.^[26]

Linked metallocenes, in particular, those with extended conjugated spacers are redox active and good candidates for the investigation of through-bond electronic communication.^[25] Ideal models consist of two or more identical metallocene units as spectators.^[22,25] It was demonstrated that acetylene bridged ferrocenes show third order *non*-linear optical properties. Furthermore, systems incorporating paramagnetic transition metal ions are good candidates for novel molecular based magnetic materials.^[32,33] Binuclear molecules based on dinickel, dicopper, and dimanganese cores, with different magnetic coupling patterns, have drawn much attention in the last decade.^[34-36]

The present work deals with the synthesis of hitherto unknown conjugated rigid ligand systems which are able to function as valuable precursors for the access to macrocycles with the potential to show electronic communication. Building blocks for the construction of these ligands are ferrocene, pyridine and its derivatives bipyridine, and phenanthroline, 1,4-diethynylbenzene, or acetylene. The synthesis and structure of three redox-active tetranuclear supramolecular rectangles bearing each two ferrocene subunits and two nickel(II), silver(I) and palladium(II) atoms, respectively, in their backbone. Furthermore four bimetallic supramolecules containing one of the bis(bidentate) ligands and one zinc(II), iron(II), or silver(I) atom, are also investigated.

2 General Section

2.1 Design of the Polydentate Ligands **1a-c**^[37,38] and **10a-d**^[38]

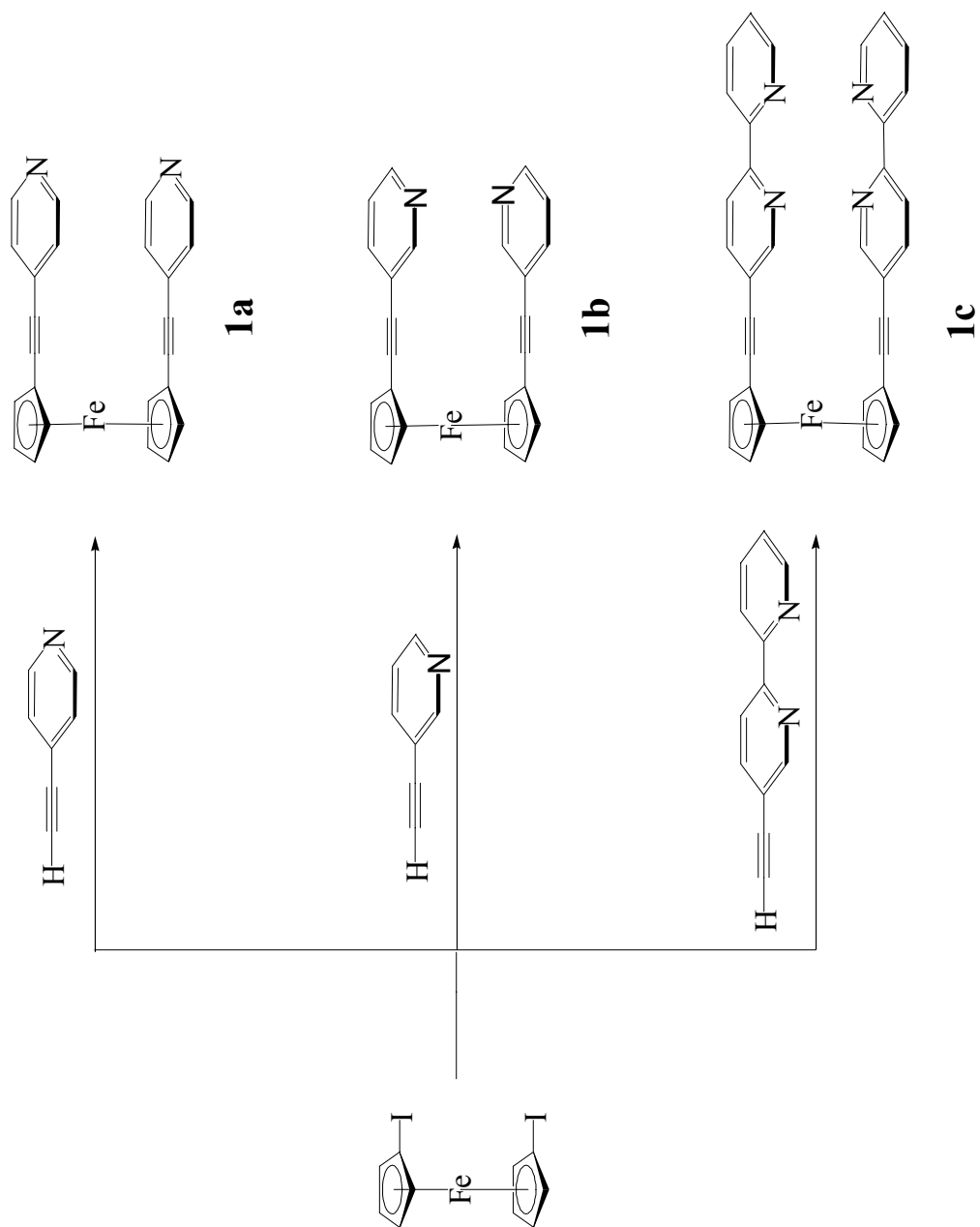
Pyridine and its derivatives 2,2'-bipyridine and 1,10-phenanthroline functionalized at positions 4,^[39] 5 or 5,5',^[40,41] and 3 or 3,8,^[42] respectively, have attracted great attention. Because of their structural characteristics they are employed in the investigation of molecular wires. 5- and 3-Ethynyl substituted 2,2'-bipyridine^[40,43] and 1,10-phenanthroline^[44,45], respectively, are important building blocks for the synthesis of materials applied in molecular electronics, because the acetylene moiety is connected to the electron rich positions of the aromatic amines. Such a unit is expected to favor through bond electronic communication. Due to mainly synthetic difficulties, only rather limited experiments have been carried out with these promising pyridine derivatives. Incorporation of these building blocks into the ligands **1a-c** and **10a-d** will make the side chains of the subunits linear and the ferrocene based ligands symmetric. Here we present the first examples of ligand systems in which a 1,1'-ferrocenediyl unit is connected to 2,2'-bipyridine and 1,10-phenanthroline at position 5 and 3, respectively, via conjugated linkers. The introduction of propoxy substituents into the *para*-position of the phenylene bridges solves the problem of low solubility.

2.2 Bis(pyridine), Bis(bipyridine), and Bis(phenanthroline) Ligands **1a-c** and **10a-d**

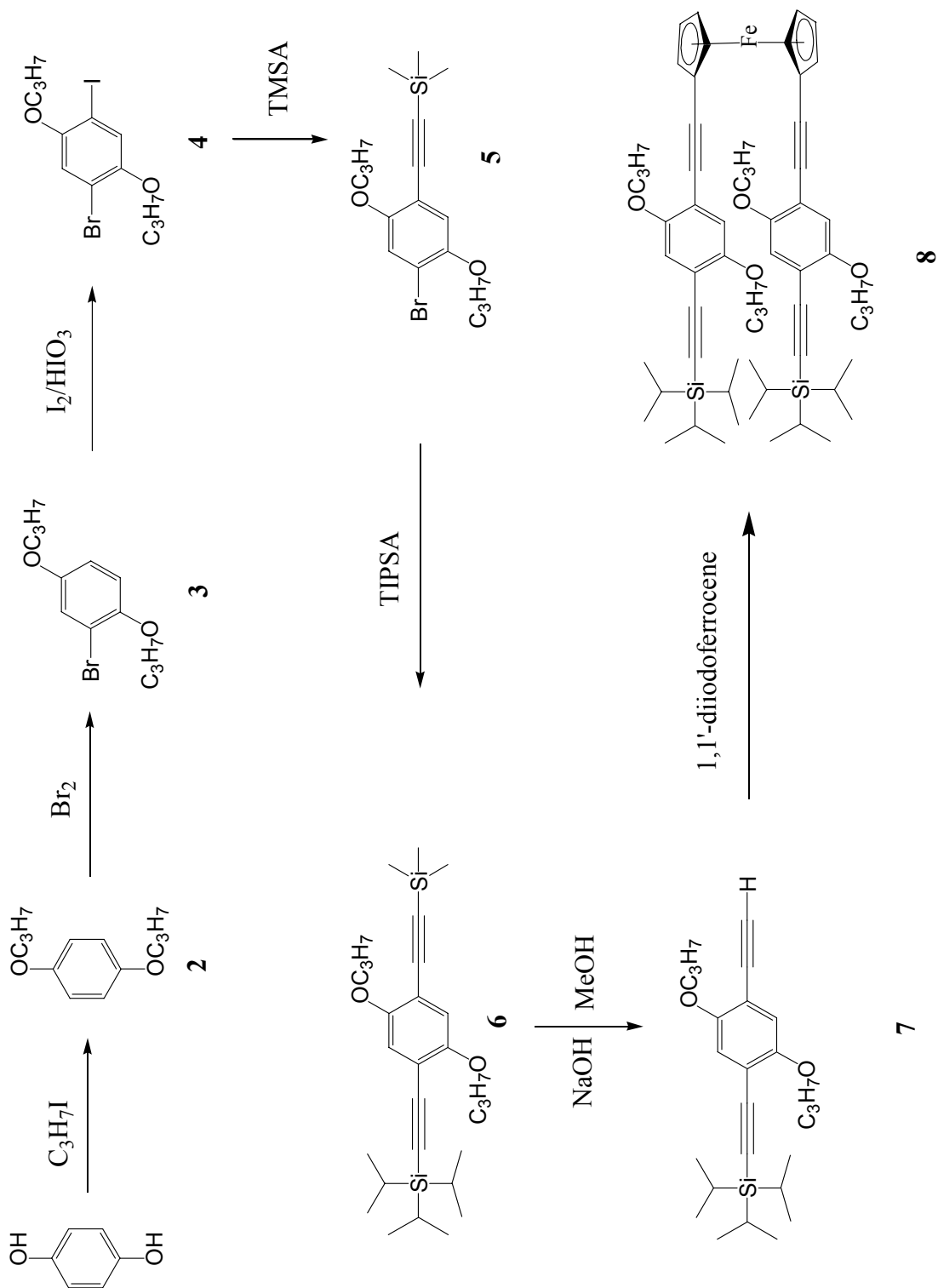
2.2.1 Syntheses of Ligands **1a-c** and **10a-d**

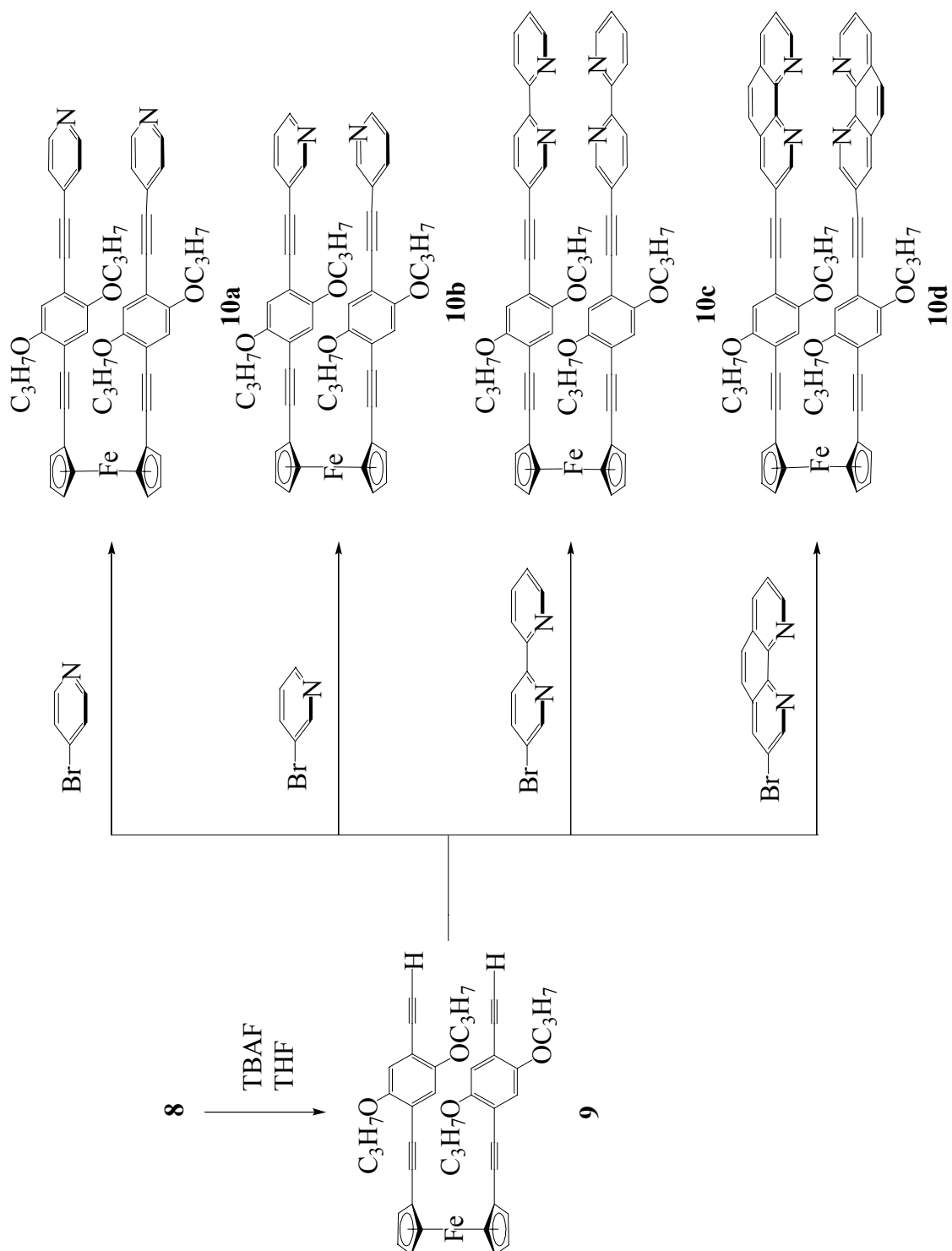
All Sonogashira C-C coupling reactions mentioned in Schemes 1-3 were promoted by either $\text{Cl}_2\text{Pd}(\text{PPh}_3)_2/\text{CuI}$ or $\text{Pd}(\text{PPh}_3)_4$ in the presence of organic amines.^[46] Ligands **1a-c** are accessible in 19-37% yields by reaction of 1,1'-diiodoferrocene^[47] with pre-organized 4-/3-ethynylpyridine^[48] and 5-ethynyl-2,2'-bipyridine^[49] in diisopropylamine as a solvent which concomitantly functions as a proton acceptor (Scheme 1). The red ligands **1a-c** are thermally and

air stable. Ligands **1a,b** are soluble in chloroform, dichloromethane, and THF, but **1c** is only slightly soluble in common organic solvents. Their molecular compositions were evidenced by EI mass spectra.

Scheme 1. Syntheses of ligands **1a-c**

A suitable way for the access of the ligands **10a-d** is the employment of the pre-constructed 1,1'-ferrocenediylbis(ethynylene) **9**. As a first step for the preparation of **9** the ferrocene derivative **8** was synthesized in 55% yield by a C-C coupling reaction^[50] between 1,1'-diiodoferrocene and 1-ethynyl-4-(triisopropylsilylethynyl)-2,5-dipropoxybenzene **7**^[51,52] in a mixture of THF and diisopropylamine (Scheme 2). Compound **7** was prepared by multi-step organic syntheses starting from hydroquinone, *via* **2**^[53] by Williamson ether synthesis, **3**^[54] by monobromination, **4**^[55,56] by monoiodination, **5**^[51] by selective coupling with trimethylsilylacetylene, and **6**^[51] with triisopropylsilylacetylene, and selective deprotection^[51,52] (Scheme 2). The intermediate **8** was characterized by mass and NMR spectroscopy as well as by elemental analyses (see Experimental part). In a following reaction, the ferrocene derivative **9** was obtained by cleavage of the triisopropylsilyl groups from **8** in the presence of tetra-*n*-butylammonium fluoride in THF at 20°C (Scheme 3).^[50] No isolation of **9** is necessary and the removal of the protecting group is performed prior to the coupling reaction with 4-bromopyridine, 3-bromopyridine, 5-bromo-2,2'-bipyridine, and 3-bromo-1,10-phenanthroline in THF-diisopropylamine. To optimize the yields of **10a-d** an excess amount of the bromo-N-heterocycles was applied. After column chromatography with silica gel and dichloromethane-methanol-THF, compounds **10a-d** are obtained as orange, air-stable powders in yields between 45 and 52%, which are soluble in chlorinated solvents and THF, but insoluble in acetonitrile, diethyl ether, or saturated hydrocarbons. The molecular compositions of **10a-d** were confirmed by FD, EI, and FAB mass spectra.

Scheme 2. Synthesis of intermediate **8**

Scheme 3. Syntheses of ligands **10a-d**

2.2.2 NMR and IR Spectroscopic Characterization of **1a-c** and **10a-d**

The polydentate nitrogen ligands **1a-c** and **10a-d** were unequivocally identified by their ^1H and $^{13}\text{C}\{^1\text{H}\}$ NMR spectra (Figures 1 and 2). Because of the high symmetry of **1a-c** and **10a-d** the protons and carbon atoms in both side chains of the ferrocene unit do not differ in their chemical shifts. Both protons in the phenylenes of **10a-d** which are unsymmetrically substituted in the *para*-position, give rise to each one singlet at ca. 7 ppm in the ^1H NMR spectra. The propoxy group is characterized by two triplets resulting from the protons of the α -methyl and γ -methylene functions and a multiplet which is assigned to the protons of the β - CH_2 unit. In CDCl_3 or CD_2Cl_2 , the cyclopentadienyl protons in **1a-c** and **10a-d** reveal an AA'XX' pattern with centers lying between 4.6 and 4.4 ppm. The α -protons in the N-heterocycles exhibit the largest chemical shifts at 8.5, 8.5, and 8.5 for **1a-c**, and 8.5, 8.7, 8.8, and 9.2 ppm in the ^1H NMR spectra of **10a-d**, respectively. All other resonances are summarized in the Experimental part.

Each ligand is provided with one (**1a,b**) or two (**10a-d**) alkyne moieties as connectors. Hence two (**1a,b**) or four (**10a-d**) different chemical shifts are found in the $^{13}\text{C}\{^1\text{H}\}$ NMR spectra located between 82 and 94 ppm. Six well resolved singlets are observed for the phenylene carbon atoms in **10a-d** in the regions 153-154 (C- OC_3H_7), 116.4-117.1(C-H), and 111.7-115.7 ppm (C1 and C4). Three ^{13}C resonances between 73 and 66 ppm in the spectra of the ligands **1a,b** and **10a-d** are attributed to the cyclopentadienyl carbon atoms. In contrast to dialkylsubstituted 1,1'-ferrocenes the *ipso*-C atoms resonate at higher field than the other carbon atoms. The assignment of the carbon atoms was supported by a DEPT-135 experiment, because in the above-mentioned region also the ^{13}C signals of the α -carbon atoms of the propoxy groups can be observed. The ^{13}C part of the N-heterocycles in **1a,b** and **10a-d** shows the expected signals for the different carbon atoms and the largest downfield shifts are ascribed to the carbon atoms adjacent to the nitrogen atoms. Carbon atoms next to the alkyne moieties give rise to ^{13}C signals at 149.8 (**1a**), 152.2 (**1b**), 131.8 (**10a**), 154.1 (**10b**), 120.6 (**10c**), and 119.3 ppm (**10d**).

A characteristic absorption in the IR spectra (KBr) of **1a-c**, and **10a-d** between 2205-2214 cm^{-1} corresponds to the $\text{C}\equiv\text{C}$ stretching vibration of the alkyne functions.

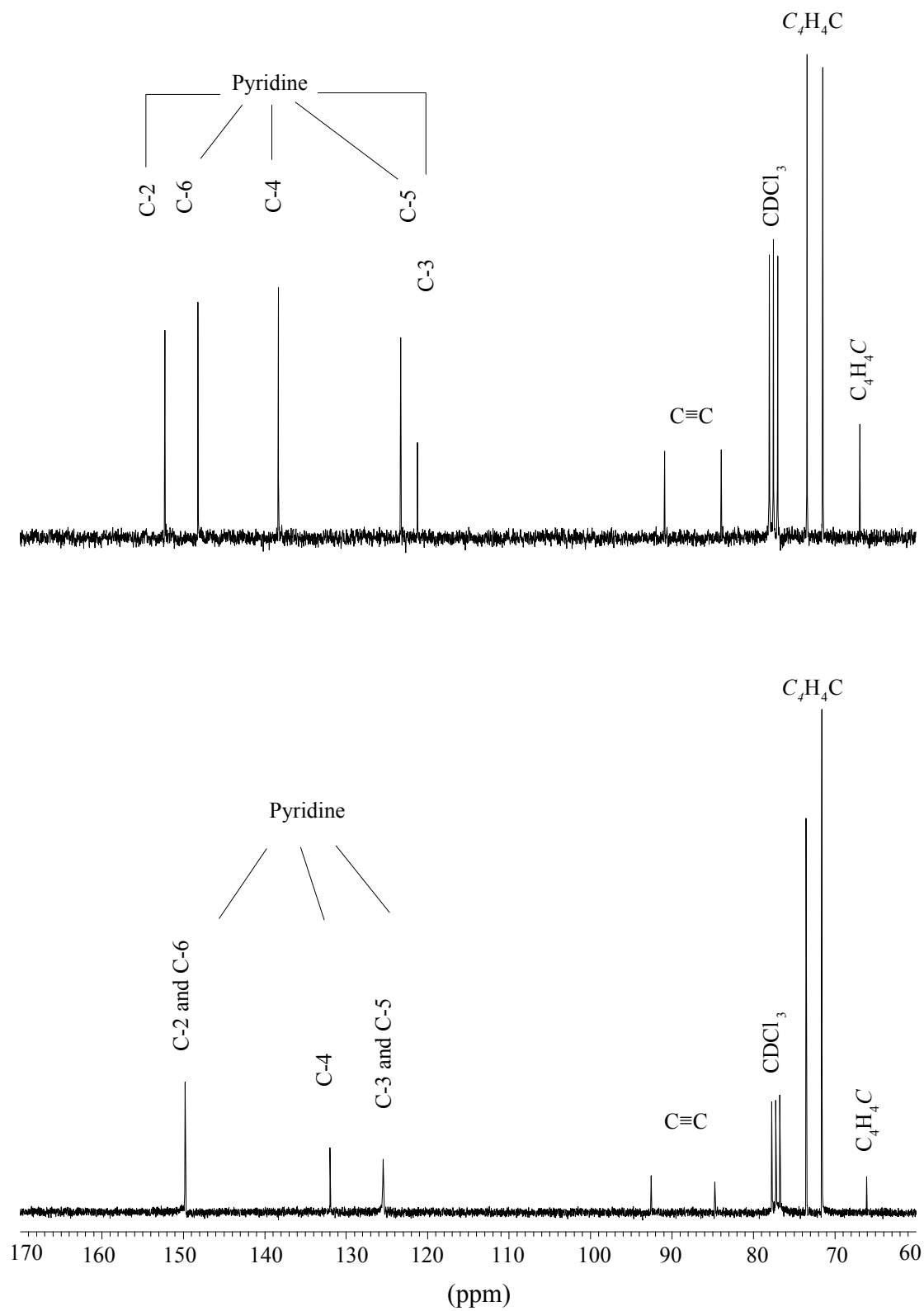


Figure 1. $^{13}\text{C}\{^1\text{H}\}$ NMR spectra of **1a** (bottom, CDCl₃) and **1b** (top, CDCl₃)

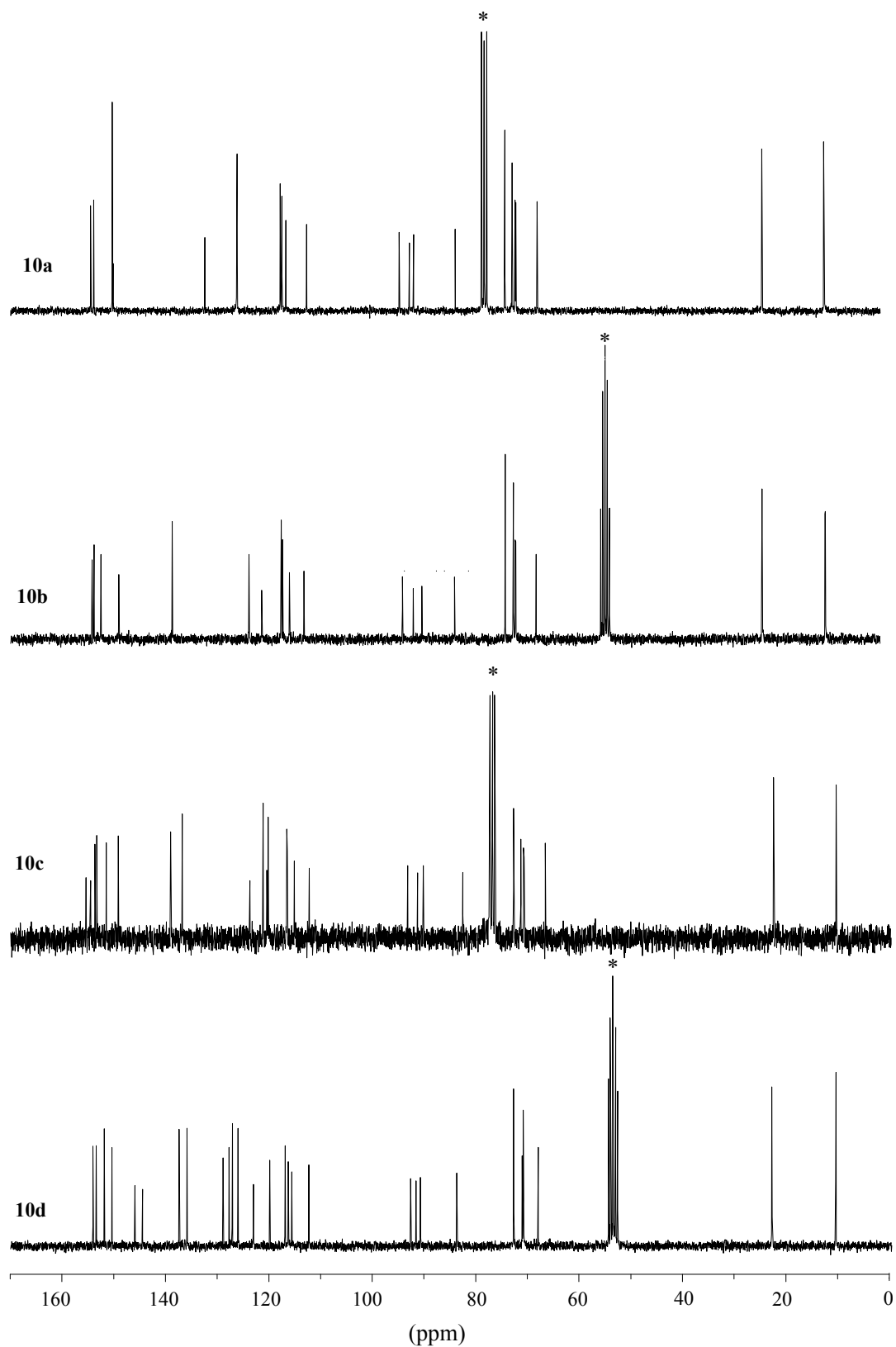


Figure 2. $^{13}\text{C}\{^1\text{H}\}$ NMR spectra of **10a** (CDCl₃), **10b** (CD₂Cl₂), **10c** (CDCl₃), and **10d** (CD₂Cl₂).

Asterisks denote solvent resonances. For peak assignments see Experimental section

2.2.3 Discussion of the Crystal Structures of **1a** and **1b**

Ligands **1a** and **1b** crystallize in the triclinic and monoclinic space groups $P\bar{1}$ and Cc , respectively. The asymmetric unit contains two (A and B of **1a**) and one (**1b**) crystallographically independent molecules. ORTEP plots of **1a** and **1b** with atom labelings are depicted in Figures 3 and 4. Tables 1 and 2 list the corresponding atomic coordinates. The iron ring-centroid distances Fe(1)-Cp(center) and Fe(2)-Cp(center) are 1.66 and 1.67/1.64 Å for **1a** and 1.66/1.66 for **1b**, respectively. Between the pyridine units the average nitrogen-nitrogen distance was found to be 3.96 Å (**1a**). While the two cyclopentadienyl rings in A and B are nearly parallel with angles of $\delta = 176.7^\circ$ (ring center-iron-ring center), the resulting dihedral angles (tilt angle α) are found to be $4.04(47)^\circ$ and $4.60(85)^\circ$. The dihedral angles between the pyridine rings in A and B show values of $5.16(47)^\circ$ and $15.85(49)^\circ$, respectively. The pyridine ring centers are separated by distances of 3.78 (molecule A of **1a**) and 3.85 Å (molecule B of **1a**) and 3.67 Å (**1b**). A significant deviation from coplanarity is observed, as revealed by tilt angles of $5.89(46)/5.60(49)^\circ$ (A of **1a**), $17.12(63)/29.20(49)^\circ$ (B of **1a**), and $16.87(79)/10.58(10)^\circ$ (**1b**) between the cyclopentadienyl ring and the attached pyridines. The torsion angles of -3.4° and 1.30° defined by C(8)-C(1)-C(13)-C(20) and C(32)-C(25)-C(37)-C(44), indicate a nearly eclipsed structure of **1a** in the solid state. It is of interest that the two side chains of **1a,b** point roughly to the same direction. This is attributed either to π - π interactions between the two side chains^[57,58] or to crystal packing forces.^[58]

A molecule of water, which is hydrogen bonded to N(1) and N(4) with O-N distances of 2.773 and 2.916 Å, respectively, is also established in the unit of **1a**. A head-to-tail disorder of molecule **1b** is found in the solid state.

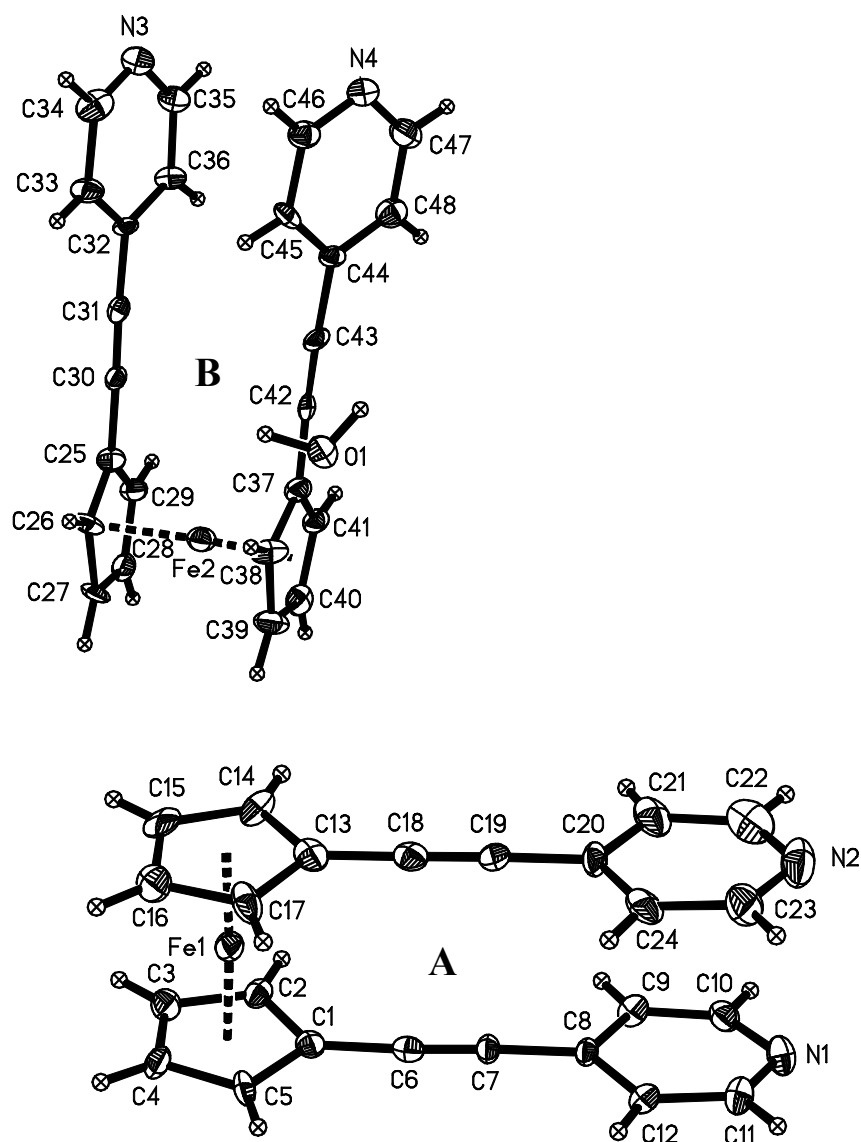


Figure 3. Crystal structure of **1a**. Selected distances (Å) and angles (deg.) for molecule A: N1-N2: 3.92; Cp(cent.)-Fe1: 1.66; py(cent.)-py(cent.): 3.78, C(6)-Cp(1)-Cp(2)-C(18): -0.3; C(8)-C(1)-C(13)-C(20): -3.4; dihedral angle: py(1)-py(2): 5.16; Cp(1)-Cp(2): 4.04

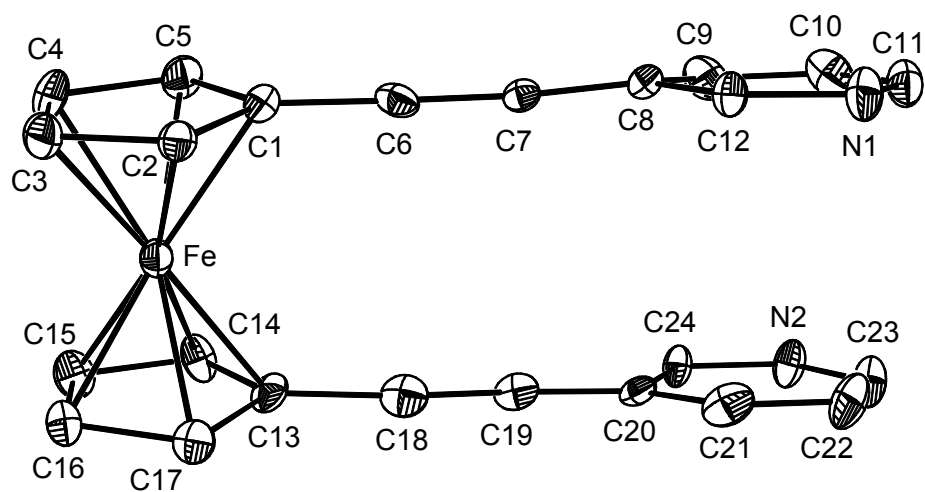


Figure 4. Crystal structure of **1b**. Hydrogen atoms omitted for clarity. Selected distances (Å) and torsion angles (deg): C3-C16: 3.21; C1-C13: 3.36; C6-C18: 3.47; C7-C19: 3.48; C8-C20: 3.61; C11-C23: 3.77, C1-C13-C20-C8: 0.78; C8-C11-C23-C20: 11.39

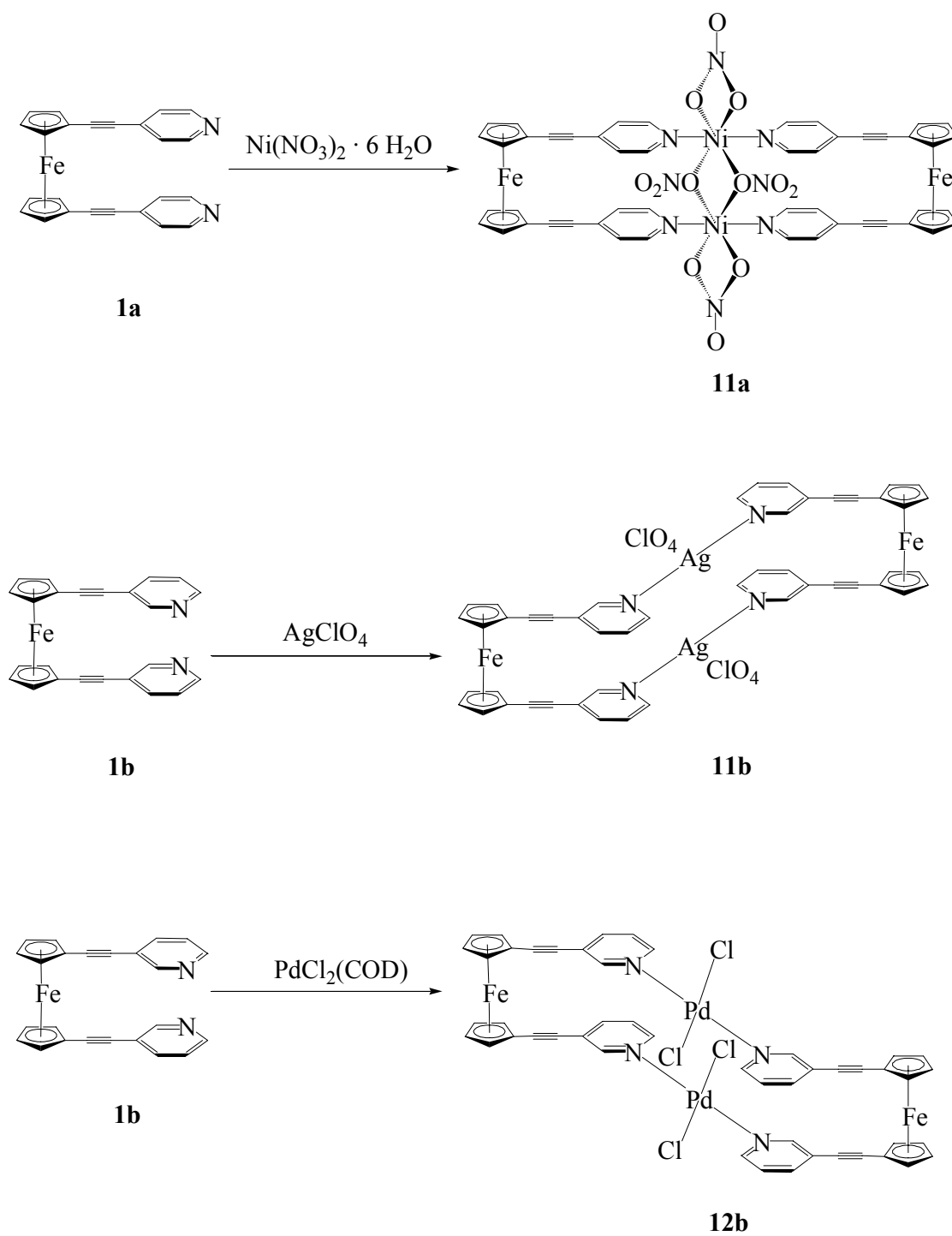
2.3 Heterotetranuclear Molecular Polygons **11a,b**^[59] and **12b**^[59]

2.3.1 Syntheses of the Macrocycles **11a,b** and **12b**

The macrocyclic motifs **11a,b** and **12b** were obtained in 92-95% yields by mixing a solution of the nitrogen donor ligands **1a** and **1b** in dichloromethane with a solution of [Ni(OH₂)₆](NO₃)₂, AgClO₄, and PdCl₂(COD) in methanol, acetonitrile, and dichloromethane, respectively, under high dilution conditions^[60] at room temperature (Scheme 4). Elemental analyses are satisfactory and consistent with their proposed structures. While the red silver compound **11b** is at least slightly soluble in polar organic media like acetonitrile, the red nickel complex **11a** shows only a very low solubility in methanol and acetonitrile. Macrocycle **12b** is insoluble in these solvents, but slightly soluble in dichloromethane and DMF. In DMF and DMSO **11a** dissolves readily under decomposition.

2.3.2 ¹H NMR and IR Spectroscopic Characterization of the Macrocycles **11a,b** and **12b**

Because of the low solubility only ¹H NMR spectra of the macrocycles **11b** and **12b** could be recorded, whereas the nickel(II) complex **11a** is paramagnetic. Upon complexation of ligand **1b** to silver(I) (**11b**) and palladium(II) (**12b**), a slight downfield shift of the pyridine protons is observed. While only the resonance at 7.05 ppm, which is assigned to H-5 of the pyridine ring in **1b**, is markedly downfield shifted to 7.20 ppm in the disilver complex **11b**, all other protons of this entity remain unchanged. In the ¹H NMR spectrum of **12b** the nitrogen adjacent protons H-2 and H-6 give rise to a remarkable down field shift of 0.18 and 0.31 ppm, respectively. On the other hand, notable upfield shifts of 0.27 and 0.31 ppm for H-4 and H-5 are observed. The AA'XX' pattern for the cyclopentadienyl rings in the spectra of **11b** and **12b** remain unchanged.

Scheme 4. Synthesis of the Macrocycles **11a**, **11b**, and **12b**

In the FT-IR spectra of **11a,b** and **12b** in particular the absorptions for the C=N and C≡C stretching vibrations are shifted somewhat to higher wave numbers compared to the free ligands **1a** and **1b**, respectively. This is consistent with the coordination of transition metals to nitrogen. Intensive bands at 1289/1218 and 1095/1050 cm⁻¹ are assigned to the stretching vibrations of the nitrate and perchlorate anions, respectively.

2.3.3 Discussion of the Crystal Structures of **11a,b** and **12b**

To obtain a detailed information about the structures of the nickel(II), silver(I), and palladium(II) containing macrocyclic complexes **11a-11b**, and **12b**, X-ray structural investigations were performed. The corresponding ORTEP plots with atom labeling are depicted in Figures 5 (**11a**) and 6 (**11b**). Atomic coordinates are shown in Tables 3 (**11a**) and 4 (**11b**). Both compounds **11a** and **11b** crystallize in the triclinic space group $P\bar{1}$ and each molecule has a center of symmetry. Complex **12b** crystallizes in the monoclinic space group $P2_1$ but has no center of symmetry. **11a** and **11b** crystallize with three CH₂Cl₂ and two CH₃CN solvent molecules, respectively. No solvent molecule has been found in the crystals of **12b**.

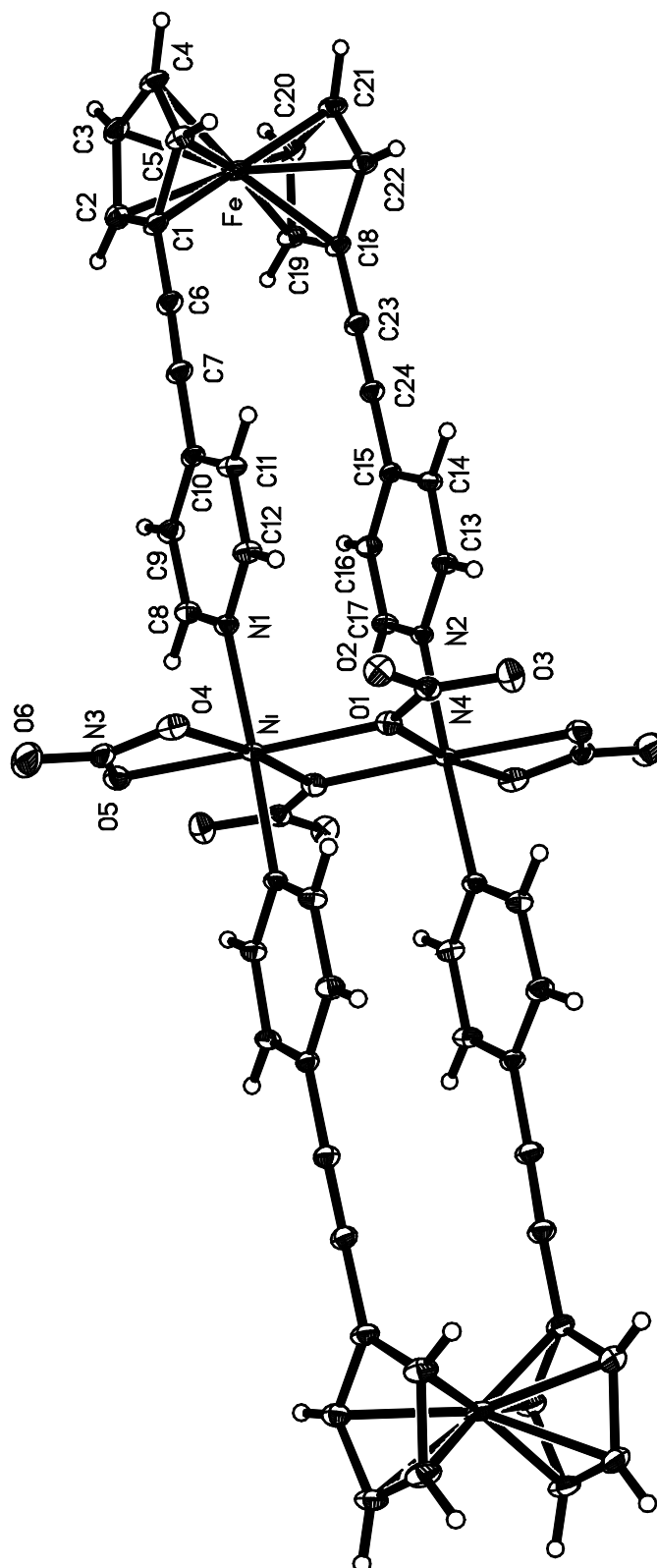


Figure 5. Crystal structure of **11a**. Selected distances (Å) and angles (deg.): Fe-FeA: 20.18, Ni-NiA: 3.39; Fe-Ni: 10.20; Fe-NiA: 10.25, Ni-O1-NiA: 107.79; N1-Ni-N2A: 176.81

Both nickel atoms in **11a** are octahedrally coordinated by two nitrogen and four oxygen donor functions, forming a *trans*-N₂O₄ coordination sphere. The two *trans*-located nitrogen atoms are equidistant from the nickel (2.05 Å), while the four Ni-O bonds are between 2.08 and 2.12 Å. However, the nickel-centered angles of the octahedron vary between 61 and 115°, indicating a considerably distorted geometry around the nickel atom.

Complex **11a** is constructed of a dinickel core with two bridging ligands **1a** [μ - η^1 : η^1 -**1a**-*N, N'*] and four nitrate counterions. The nitrates are coordinated in two different modes to the nickel centers. Two of them function as μ_2 -bridging ligands, whereas the other two are η^2 -chelated. Within a ligand **1a** in complex **11a**, the N-N distance of 3.49 Å is significantly shorter than the corresponding average distance of 3.96 Å in the free ligand **1a**, in which the repulsion of the nitrogen lone pairs has to be considered.

Concerning the dinickel core the structure of **11a** can be designated as an unsymmetric paddlewheel consisting of the coordinated nitrates and two moieties of ligand **1a**. The whole structure has the shape of a molecular rectangle in which the four Cp rings occupy the vertices, whereas the four metals are located in the middle of the edges. The lengths of the edges are 3.31 and 20.24 Å, calculated from the center points of the cyclopentadienyl rings. Both nickel and iron atoms are separated by a distance of 3.39 and 20.18 Å, respectively. In this molecule the four metal atoms are lying in a plane, creating almost a regular rhombus with lengths of 10.20 (Fe-Ni) and 10.25 Å (Fe-NiA) and angles of 19° (Ni-Fe-NiA) and 161° (Fe-Ni-FeA). One of the most important structural features of **11a** is the coplanarity of the entire inorganic entity (nickel atoms and all four nitrates). The ferrocene units are positioned above and below this plane. In the solid state, molecules of **11a** are offset positioned and separated by dichloromethane molecules (Figure 7). The dinickel cores are lined up along the *b* axis with dichloromethane in between. There are two kinds of crystallographically independent dichloromethane molecules, which are hydrogen bonded to the nitrate anions in two modes. The dichloromethane molecules on the *bc* plane use just one of their hydrogen atoms to interact with oxygen of a μ_2 -nitrate (H(40B)-O(3), 2.55 Å),

whereas both hydrogen atoms of dichloromethane on the *ab* plane show H-bondings to oxygen atoms of a μ_2 -nitrate (H(41B)-O(2), 2.42 Å) and an η^2 -nitrate (H(41A)-O(6), 2.49 Å), respectively. As a consequence of the hydrogen bonds, each type of the dichloromethane molecules is head-to-head oriented.

Due to the 3-position of the nitrogen donors in ligand **1b** and the preferred coordination number two for silver(I), the structure of the cation **11b** is somewhat different from that of **11a**. The former constitutes at most a distorted rectangle defined by the central points of the four cyclopentadienyl rings (Figure 6). If a connecting line is drawn between these points, one pyridine is located before and the other one behind this line. The dimensions of the rectangle are 17.42 and 3.31 Å. All four transition metals (each two silver and iron metals) are lying in a plane and the Fe-Fe and Ag-Ag distances are 17.34 and 3.50 Å, respectively. The heteroatom distances (Ag-Fe) are 8.65 and 9.03 Å. Similar to complex **11a**, in **11b** silver is nearly equidistant to the two coordinated pyridine N-atoms (2.170(2) and 2.179(2) Å). Only a slight deviation from a linear N-Ag-N arrangement is observed (178.1°).

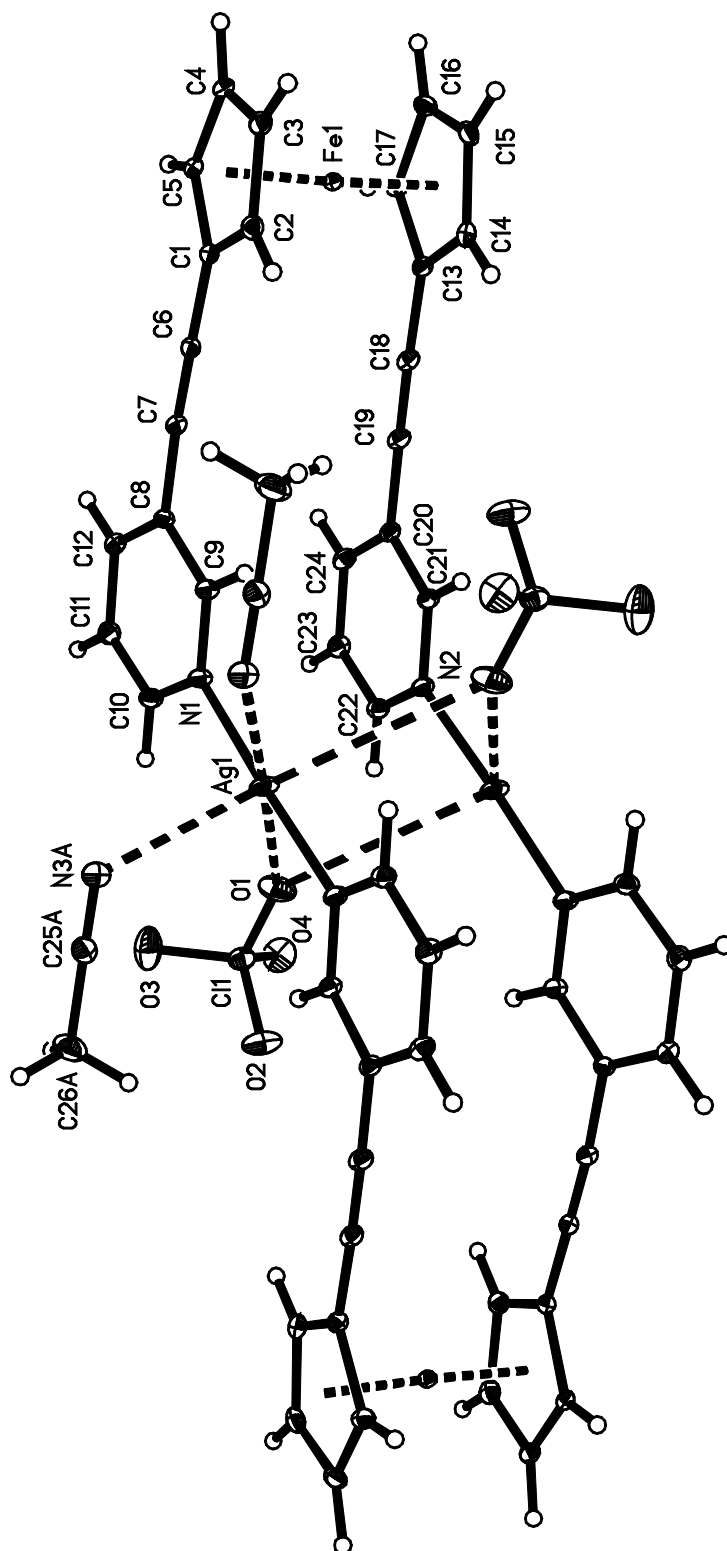


Figure 6. Crystal structure of **11b**. Selected distances (Å) and angles (deg.): Fe1-Fe1A: 17.34; Ag1-Ag1A: 3.50; Fe1-Ag1: 8.65; Fe1-Ag1A: 9.03, N1-Ag1-N2A: 178.1

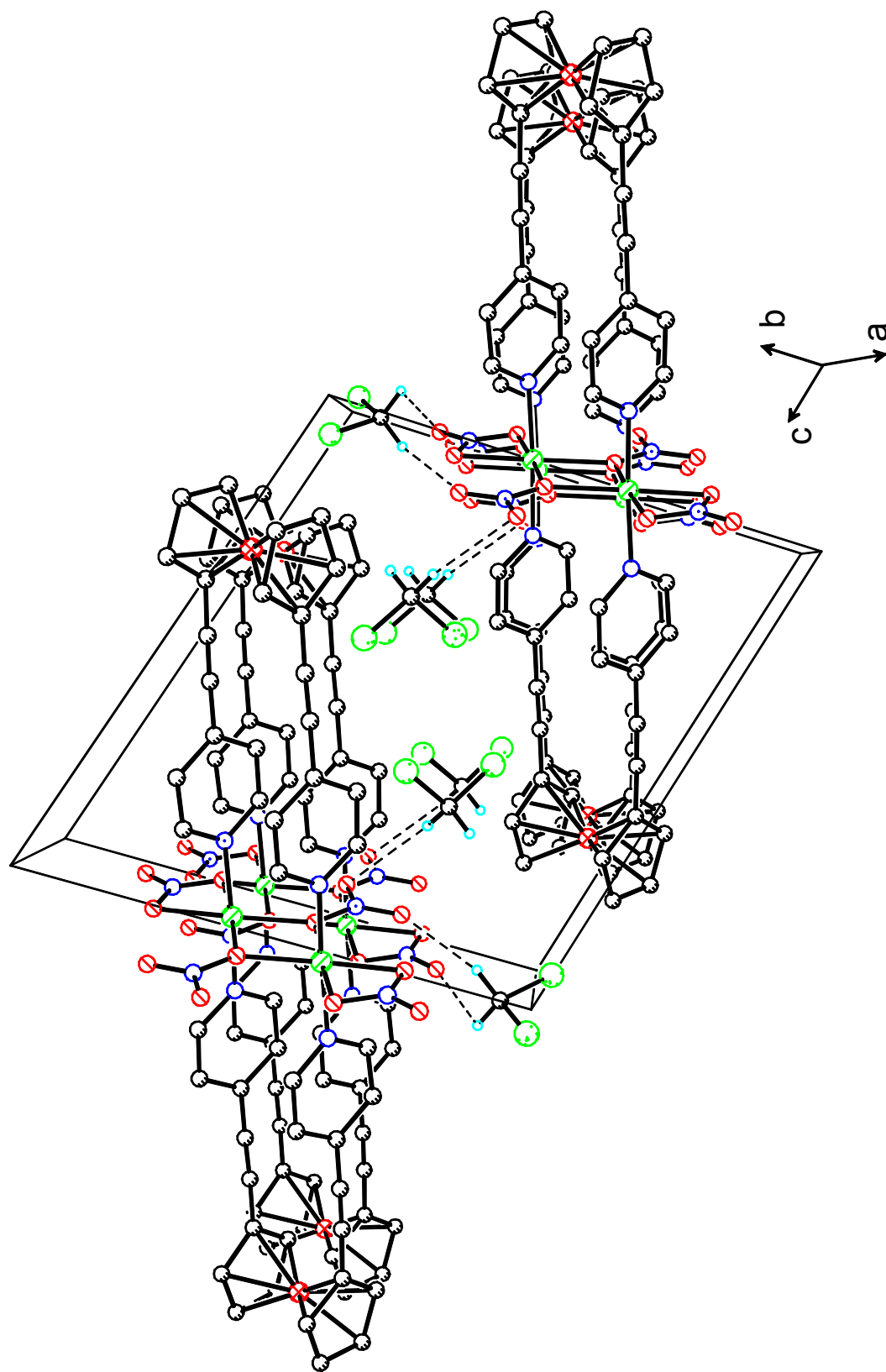


Figure 7. Molecular packing of **11a** showing the offset arrangement of molecule **11a**, the hydrogen bonds, and head-to-head orientation of the dichloromethane molecules

Both perchlorate anions are positioned on each side of the rectangular plane and function as *pseudo*-bridges for the disilver core with Ag-O distances of 2.79 and 3.74 Å and oxygen and silver centered angles of 117.2 and 62.8°, respectively (Figure 6). In the solid state the molecules of **11b** are layered and acetonitrile is located between these rectangular molecules (Figure 8). The acetonitriles function as bridging ligands and intermolecularly connect two silver cations forming a parallelogram. The macrocycles are held together by weak acetonitrile-silver interactions with Ag-N distances of 2.705(2) and 2.891(2) Å, forming a supramolecular framework. Concerning also the weak interactions each silver atom can be regarded as *pseudo*-octahedrally coordinated by four nitrogen and two oxygen atoms in a *cis*-N₄O₂ fashion. In the center of each macrocycle, a parallelogram is generated by each two silver and oxygen atoms. Both the inter- (Ag₂N₂) and intramolecular (Ag₂O₂) parallelograms are nearly coplanar and deviate by an angle of 17.5°. The two CpC₂py arms on each side of the macrocycle are not exactly oriented parallel, deviations with respect to Cp/py and py/py are 6.1/13.1 and 6.2°, respectively. Of particular interest is the parallel alignment of the silver atoms along the *a* axis with intra- and intermolecular Ag-Ag distances of 3.50 and 3.79 Å, respectively. Each of the other components (ferrocene, perchlorate and acetonitrile) is also aligned along the *a* axis.

Due to the low quality of the crystal of **12b**, only a brief information is given. An isotropical ball and stick plot with selected atom labeling is shown in Figure 9. The molecular structure of **12b** is similar to that of **11b**, but no center of symmetry is present. In addition, each palladium atom is additionally coordinated to two *trans*-positioned chlorides with PdCl₂ units about 45° to the pyridine rings. Intermetallic distances are 17.606(7) for Fe1-Fe2, 4.117(2) for Pd1-Pd2, 8.927(7) for Pd1-Fe1, 9.130(6) for Pd1-Fe2, 9.146(6) for Pd2-Fe1, 8.959(6) for Pd2-Fe2, 3.118(8) Å Pd2-Cl1. Selected angles are 140.5(3) for Cl2-Pd1-Pd2 and 48.8(2) degree for Cl1-Pd1-Pd2.

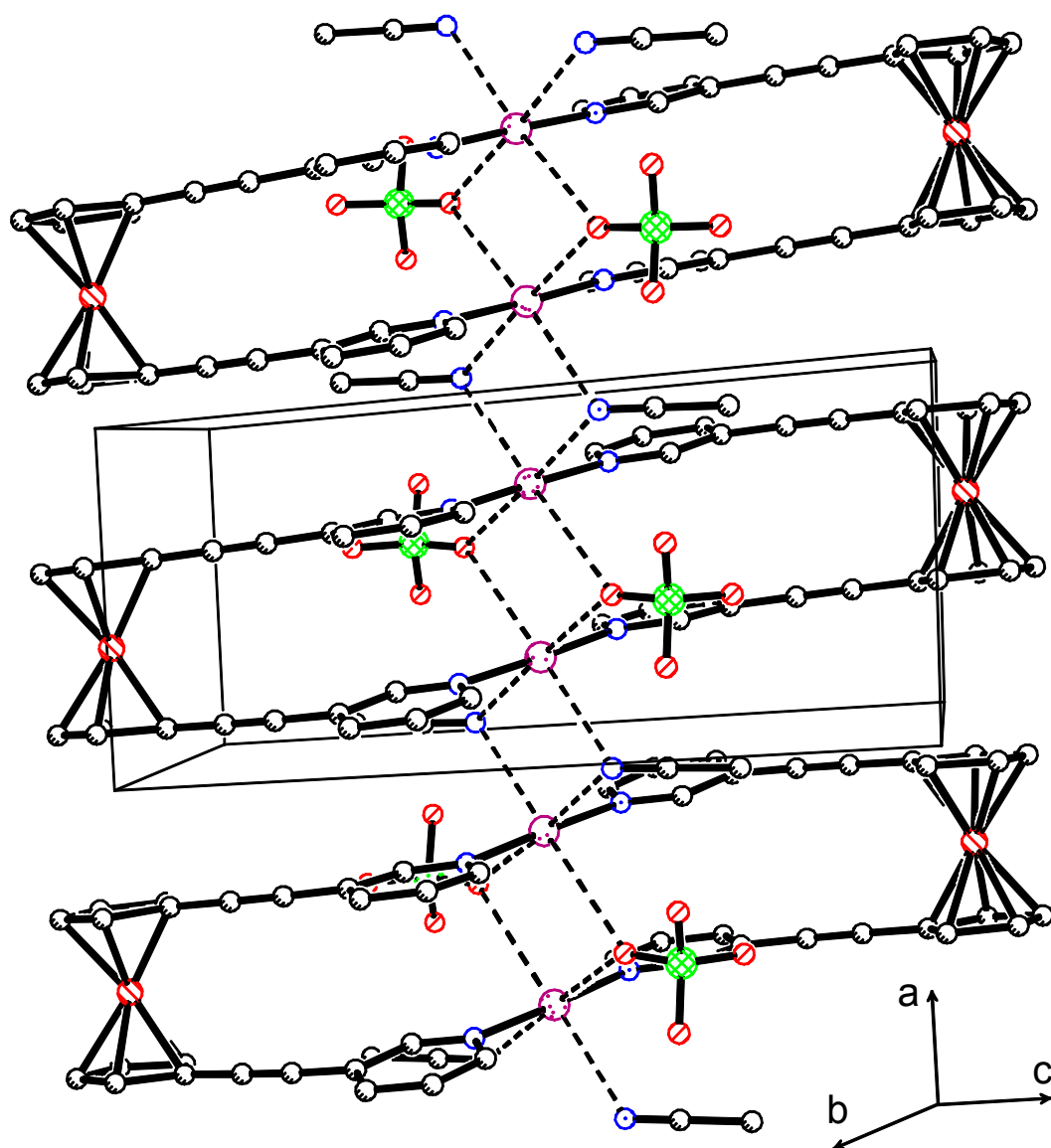


Figure 8. Molecular packing of **11b** along the *a* axis presenting the parallel alignment of the silver ions and the other components as well as the alternating intramolecular Ag_2O_2 and intermolecular Ag_2N_2 parallelograms

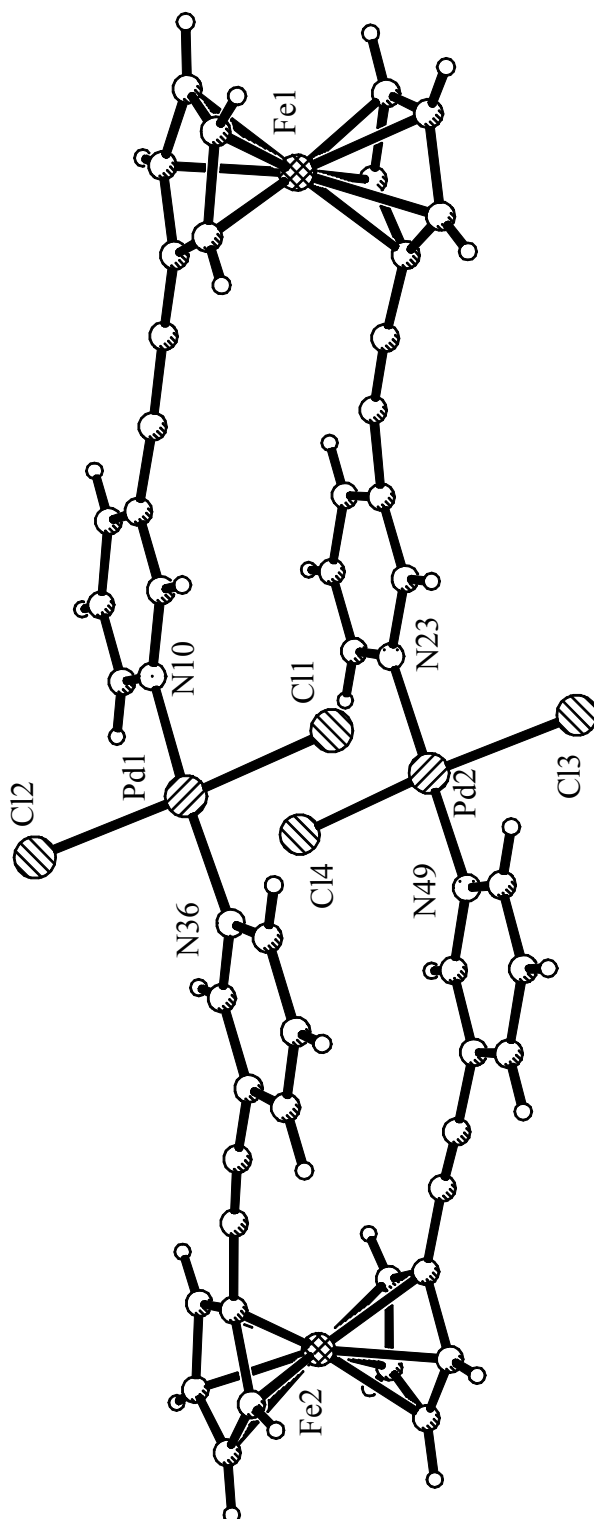


Figure 9. Molecular structure of **12b**. Selected distances (Å) and bond angles (deg.): Fe1-Fe2: 17.61; Pd1-Pd2: 4.12; Pd1-Fe1: 8.93; Pd1-Fe2: 9.13; Pd1-N10: 2.04; Pd1-N36: 2.01; Pd1-Cl1: 2.34; Pd1-Cl2: 2.40; Pd2-Cl1: 3.12, N10-Pd1-N36: 172.4; Cl1-Pd1-Cl2: 170.6; N10-Pd1-Cl1: 89.7; N36-Pd1-Cl2: 89.0; Cl1-Pd1-Pd2: 48.8; Cl4-Pd2-Pd1: 51.1

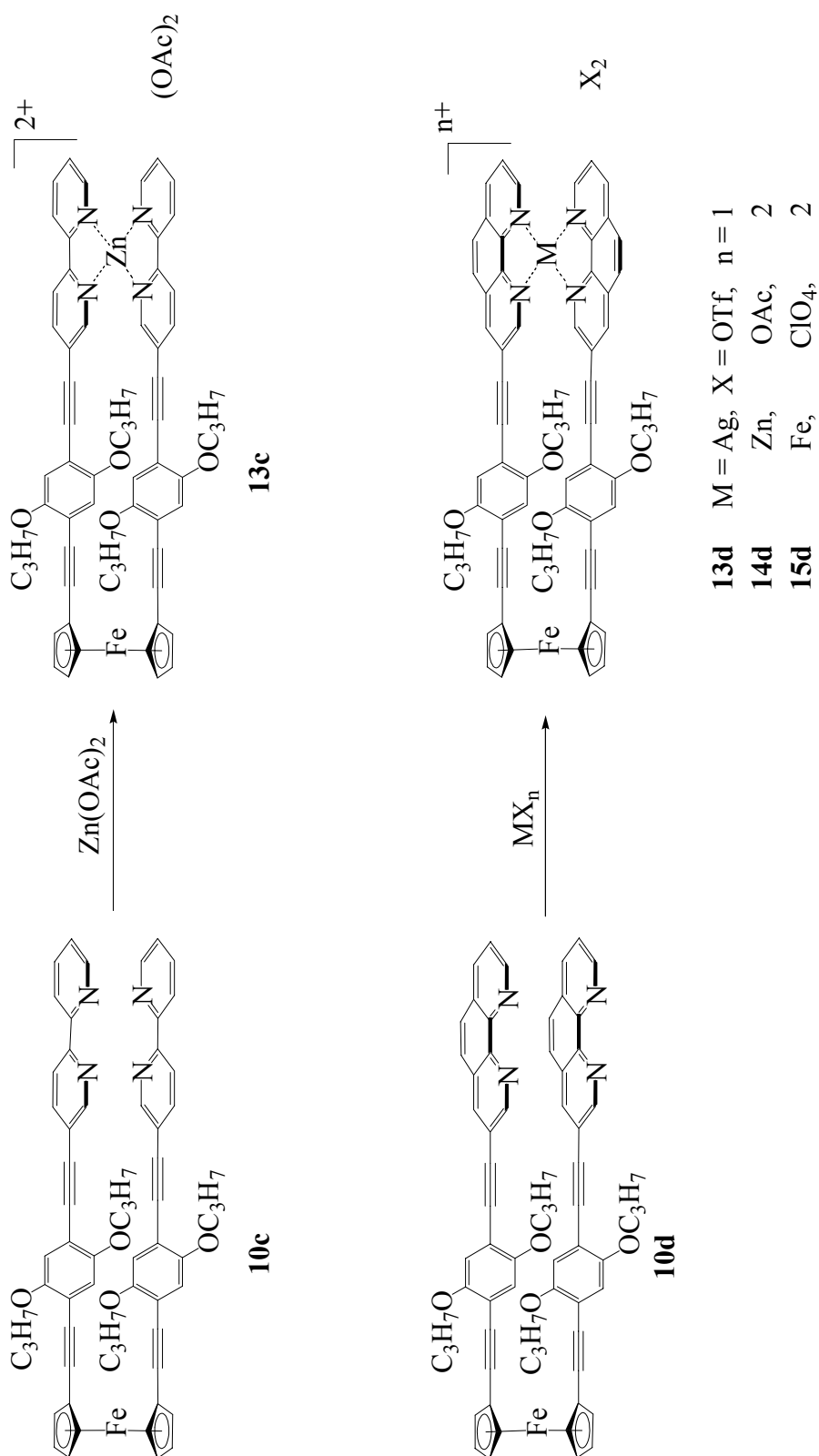
2.4 Binuclear Macrocycles **13c**, **13d**, **14d**, and **15d**

2.4.1 Syntheses and Properties of **13c**, **13d**, **14d**, and **15d**

These bimetallic complexes were prepared in 80-95% yields by slowly adding a solution of stoichiometric amounts of $\text{Zn}(\text{CH}_3\text{COO})_2 \cdot 2 \text{H}_2\text{O}$, AgCF_3SO_3 , or $\text{Fe}(\text{ClO}_4)_2 \cdot 6 \text{H}_2\text{O}$ to a chloroform solution of **10c** or a dichloromethane solution of **10d** at room temperature (Scheme 5). They are red to dark red solids and somewhat soluble in dichloromethane and chloroform, but insoluble in ether and saturated hydrocarbons. No melting points were detected up to 350°C.

2.4.2 ^1H NMR, MS, and IR Spectroscopic Characterization of **13c**, **13d**, **14d**, and **15d**

FAB-MS spectra confirmed the molecular compositions corresponding in each case to the loss of one counter anion (silver(I) complexes), one and two counter anions (zinc(II) and iron(II) complexes) from the expected 1:1 composition,^[1-4,6] whereas the signals of the dimeric 2:2 silver complex could only be detected in traces.^[3,6] Elemental analyses are satisfactory and consistent with the proposed structures. Their ^1H NMR spectra are characterized by the disappearance of the coupling patterns^[6] in each of the aromatic subunits (Figure 10). Peak broadening, which was associated with the twist motion^[6] of the complexes and the loss of symmetry hence generating the magnetic inequivalence of the protons, is found. Downfield shifts of 0.07 of the H-6 (**13c**) and 0.12 of H-2 (**13d**) resonances from 8.80 (**10c**) and 9.13 ppm (**10d**), respectively, are observed, in contrast to the upfield shifts of 0.47 ppm (**15d**). The resonances of the cyclopentadienyl and propoxy protons in the complexes **13c-d** remain almost unchanged, while upfield shifts of 0.91 ppm of the alpha-protons in the propoxy group and 0.16/0.04 ppm of the Cp protons in **14d** are observed, compared with those in the free ligands. Significant upfield shifts of the phenyl (0.05 - 0.82 ppm) protons are also found in the complexes **13c-d**, **14d**, and **15d**. No $^{13}\text{C}\{^1\text{H}\}$ NMR spectra are recorded, because of the limited solubility of these complexes. The $\text{C}\equiv\text{C}$ stretching vibrations are located at about 2203 cm^{-1} in the IR spectra of **13d**, **14d**, and **15d**, and at 2215 cm^{-1} in the case of **13c**, in addition to the peaks of the anion.

Scheme 5. Syntheses of Macrocycles **13c**, **13d**, **14d**, and **15d**

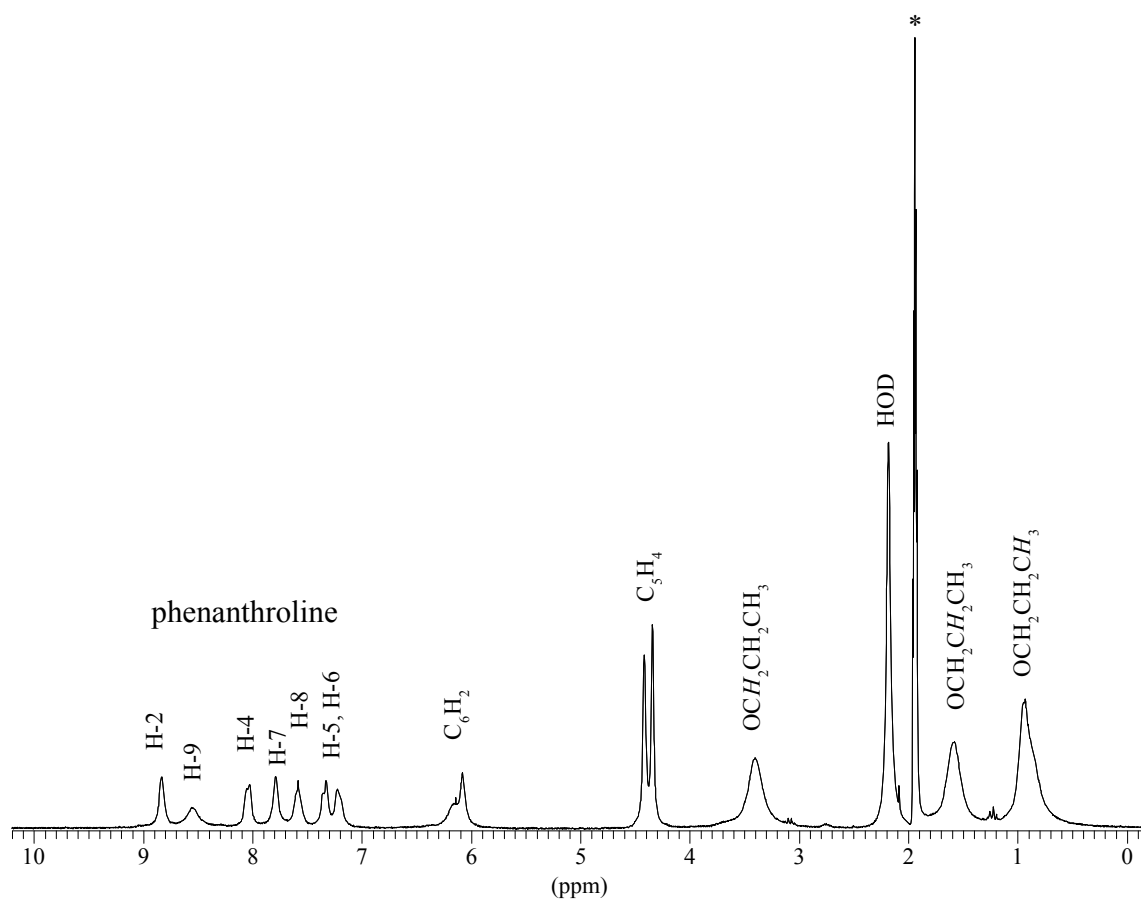


Figure 10. ^1H NMR spectrum of **14d**. Asterisk denotes solvent resonance

2.5 Electrochemical Investigations

The redox properties of compounds **1a,b** and **11a,b** were investigated in acetonitrile. The low solubility of the palladium complex **12b** prevents any studies of its electrochemical behavior. Although the ferrocene-based redox reactions of **1a,b** and **11a,b** are chemically reversible in each case, their electrochemistry is somewhat different. While ligand **1b** shows a diffusion controlled one electron transfer reaction, the response of ligand **1a** is diffusion controlled and dependent on the rate of electron transfer. Isomeric ligands **1a** and **1b** show different redox potentials at 318 and 283 mV relative to that of ferrocene/ferrocenium, respectively. They are more difficultly oxidized than the unsubstituted parent ferrocene which is traced back to the electron-withdrawing nature of

the substituents at the Cp rings. However, the difference of 35 mV between **1a** and **1b** indicates the influence of the charge distribution on the transfer of this effect. Although both ferrocene subunits of complex **11a** are oxidized at the same potential, it reveals a 32 mV positive shift related to ligand **1a**. This finding demonstrates a successful electron transfer from ferrocene to the nickel atoms, but no communication between the two ferrocenes.

Compared to ligand **1b** a negative shift of 10 mV was established for the disilver complex **11b**. This effect is usually not expected and is supposedly due to the weak σ electron acceptor and strong π donor capabilities of silver(I).^[61] As a result of this back bonding and/or the charge distribution order the ferrocene moieties are easily oxidized. Figure 11 presents the cyclic voltammogram of complex **11b**, the electrochemical response of which is diffusion controlled, whereas that of the dinickel complex **11a** is more complicated due to its adsorption character.

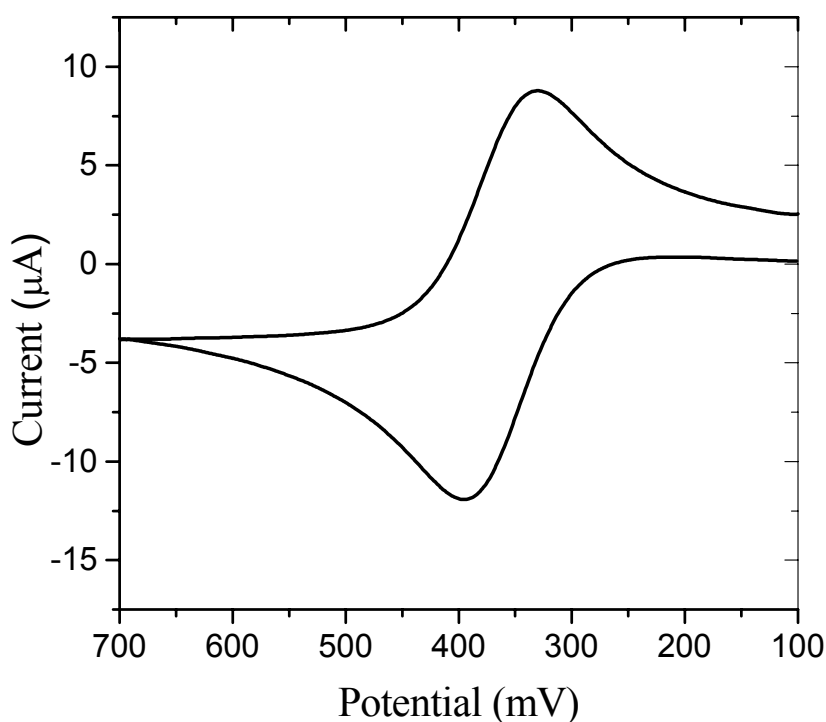


Figure 11. Cyclic voltammogram of **11b**

For a possible electronic communication between the two ferrocene units the intramolecular iron-iron distances (**11a**: 2.0 nm; **11b**: 1.7 nm) are of importance. Because of the well separated ferrocene building blocks coulombic interaction (through space electronic coupling) is neglectable. On the other hand, the alignment of the molecular orbitals^[20] and the extent of conjugation^[24] could be a reason for through bond electronic communication as it was observed in a conjugated alkyne-bridged rhenium(II) complex.^[23] In spite of these favorable preconditions no electronic communication was found in complexes **11a** and **11b**.

The half wave potential of **10a** (203 mV) measured in dichloromethane is 115 mV less positive than that of its smaller analogue of **1a**, showing clearly that the influence of the pyridine-4-yl entity on the ferrocene subunit is weakened due to the longer bridges in **10a**. Ligand **10d** shows a half wave potential of 166 mV relative to that of ferrocene in dichloromethane. No remarkable difference between the cyclic voltammetric responses of the bimetallic complex **15d** and ligand **10d** has been observed, indicating the lack of electronic interaction between the two linked metal atoms.

2.6 Magnetic Investigation of Complex 11a

The magnetic properties of the dinickel complex **11a** were studied at 10 T in the temperature range between 300 to 5 K. Experimental data obtained for the molar susceptibility and the calculated effective magnetic moment are plotted in Figure 12. The general isotropic spin-Hamiltonian expression for the symmetrical dinickel compound is $\mathbf{H} = -JS_{\text{A}} \cdot S_{\text{B}}$ ($S_{\text{A}} = S_{\text{B}} = 1$), where J represents the coupling constant between the two nickel(II) atoms. Although no maximum for χ_{M} in Figure 12 has been found in the selected temperature range, a non-linear fit of the experimental data for the susceptibility per nickel dimer using literature-known expressions^[36] yields the following values: $g = 2.22 \pm 0.01$, $J = -17.37 \pm 0.24 \text{ cm}^{-1}$, $D = 7.87 \pm 0.17 \text{ cm}^{-1}$, and $p = 17.6 \pm 0.1\%$. The g value is reasonable for octahedrally coordinated nickel(II),^[35] and the coupling constant reveals a weak antiferromagnetic interaction between the intramolecular nickel(II) atoms.

This coupling for the bis(μ -oxo) bridged dinickel(II) complex **11a** with a Ni-Ni distance of 3.39 Å is more significant than that observed for other dinickel complexes in which two bridges consisting of two or more atoms are present and both nickel units are separated by distances between 4.16 and 4.32 Å,^[35] however, clearly weaker than that of cyano-bridged dinickel complexes.^[34] Complex **11a** is impurified by an uncoupled paramagnetic species which is a chain-like polymer or oligomer^[62] formed even under high dilution conditions. They could not be separated from **11a**, because both entities show very low solubility. The agreement factor $R = 9.8 \cdot 10^{-5}$ shows that the curve is well fitted.

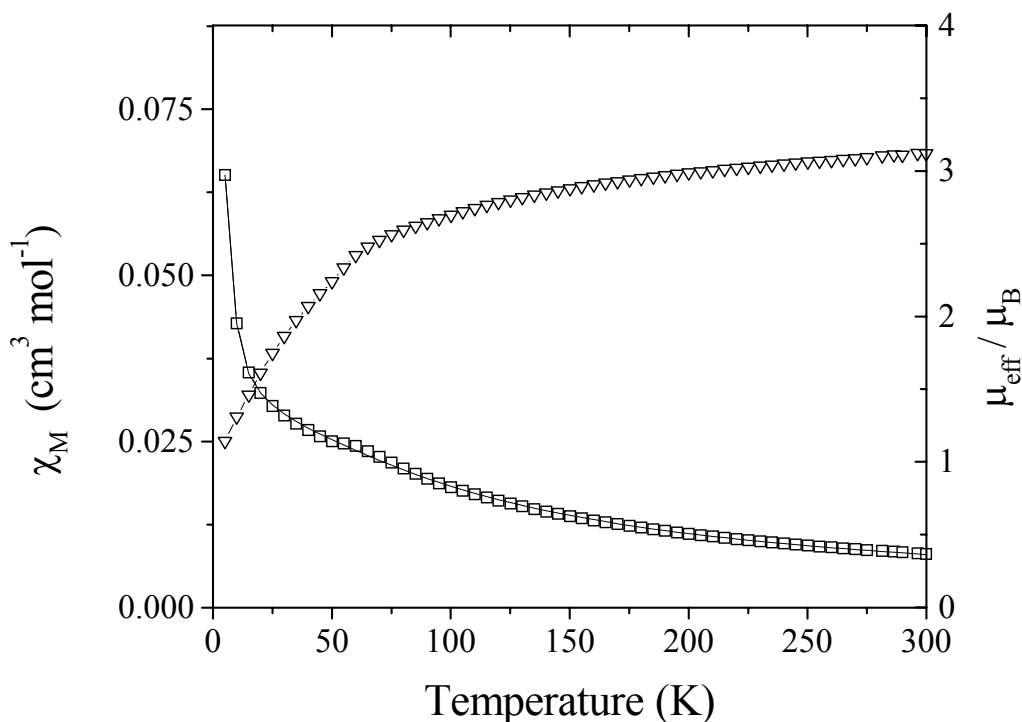


Figure 12. Temperature dependence of the magnetic susceptibility (square, left scale) and effective magnetic moment (down triangle, right scale) of **11a**; the solid lines represent the best-fit curve

2.7 Conclusion

1,1'-Ferrocenediyl bridged bis(pyridine), bis(2,2'-bipyridine), and bis(1,10-phenanthroline) ligands belong to a family of building blocks for the investigation of electronic communication.^[1-8] In contrast to previous ligands of this kind,^[1-8] **1a-c** and **10a-d** represent a novel generation with some unique characters: (a) the linkers are rigid and conjugated; (b) isomers **1a/1b** and **10a/10b** are prepared for comparison; (c) 2,2'-bipyridine and 1,10-phenanthroline are connected at much less common positions 5 and 3, respectively. In order to connect two N-heterocycles with two cyclopentadienyl rings of a 1,1'-ferrocene entity with acetylene or *para*-phenylene ethynylene linkers, two synthetic strategies have been developed and discussed. The first one is featured by pre-constructed terminal ethynyl-N-heterocycles, while the second one refers to the pre-organized 1,1'-ferrocenediylbis(acetylene) derivative **9**. Both of the approaches have been successively applied for the syntheses of the ligands **1a-c** and **10a-d**, respectively. The introduction of propoxy substituents into the *para*-position of the phenylene bridges solves the problem of low solubility. The parallel (eclipsed) arrangement of the side chains in the crystal structures of **1a,b** is ascribed to π - π interactions and/or crystal packing forces, which play an important role in the formation of transition metal complexes.

Functionalized heterotetranuclear regular (**11a**) and distorted (**11b**, **12b**) rectangles bearing two redox active ferrocene subunits and a pair of transition metals each were made accessible by coordination-driven spontaneous self-assembly. Although silver is considerably bigger than nickel, the separation between the two equal transition metal atoms in the dimetallic Ag₂ and Ni₂ cores is rather similar (3.50 vs 3.39 Å). This behavior is mainly controlled by the kind of the employed ligands **1a** and **1b**. Due to the different positions of the nitrogen atoms in ligands **1a** and **1b**, the molecular structure of **11a** is an ideal rectangle, whereas **11b** and **12b** reveal deformed rectangles. No long-distance through bond electronic communication was established in the macrocyclic complexes **11a** and **11b**. Mainly two factors should be responsible for this observation. Both ferrocene building blocks are separated by a distance of more than 1.7 nm, thus too far away to

communicate. Moreover the Ni₂ and Ag₂ core fail to transmit the Cp-C≡C-py conjugation.^[17] However, a weak influence of the Ni(II) and Ag(I) atoms through the conjugated bonds on the redox potential of the ferrocene units has been established in spite of a distance of 1 nm. No such interaction has been electrochemically established in the bimetallic complexes. In the case of the nickel(II) complex **11a** a weak antiferromagnetic interaction between the intramolecularly arranged nickel(II) atoms was found.

3 Experimental

3.1 General Considerations

3.1.1 Working Procedures

All reactions and manipulations were carried out under an atmosphere of argon by use of standard Schlenk techniques except otherwise noted. Solvents were dried with appropriate reagents, degassed, and stored under argon.

3.1.2 Characterization

FT-IR data were obtained with a Bruker IFS 48 FT-IR spectrometer. FD and FAB mass spectra were recorded on a Finnigan MAT 711 A (8 kV) instrument, modified by AMD and EI mass spectra were performed on a Finnigan TSQ 70 (70 eV, 200°C) instrument. ^1H and $^{13}\text{C}\{^1\text{H}\}$ NMR spectra were recorded at 25°C on a Bruker DRX 250 spectrometer operating at 250.13 and 62.90 MHz, respectively. ^1H and ^{13}C NMR chemical shifts were referenced to partially deuterated and deuterated solvent peaks, which are reported relative to TMS. Elemental analyses were carried out with an Elementar Vario EL analyzer.

3.1.3 Starting Materials

1,1'-diiodoferrocene,^[47] 5-bromo-2,2'-bipyridine,^[63] 3-bromo-1,10-phenanthroline,^[42] 4-/3-ethynylpyridine,^[48] 5-ethynyl-2,2'-bipyridine,^[49] tris(2-pyridyl)phosphine,^[64] Pd(COD)Cl₂,^[65] Pd(PPh₃)₄,^[66] Pd(PPh₃)₂Cl₂,^[67] and compounds **2**,^[53] **3**,^[54] **4**,^[55,56] **5**,^[51] **6**,^[51] and **7**,^[51] were synthesized according to literature or modified literature methods. AgClO₄, Ni(NO₃)₂ · 6 H₂O and other chemicals were from commercial sources and used without further treatment.

3.2 Preparation of the Compounds

3.2.1 General Procedure for the Synthesis of **1a-c**

To a solution of 1,1'-diiodoferrocene (440 mg, 1.0 mmol) and 4-/3-ethynylpyridine (257 mg, 2.2 mmol) or 5-ethynyl-2,2'-bipyridine (400 mg, 2.2 mmol) in diisopropylamine (20 mL), Pd(PPh₃)₂Cl₂ (28 mg, 0.04 mmol) and CuI (19 mg, 0.1 mmol) were added. The mixture was refluxed at 80-85°C for 2 d. Then the solvents were removed in vacuo and the residue was treated with 100 mL of a 1:1 mixture of water and dichloromethane (**1a,b**) or chloroform (**1c**). The organic extract was dried over magnesium sulfate. Column chromatography was conducted with silica gel and 0-5% methanol/THF in dichloromethane. Recrystallization from dichloromethane/acetonitrile afforded **1a,b**.

3.2.1.1 1,1'-Bis(4-pyridylethynyl)ferrocene (**1a**)

Yield (128 mg, 33%), air stable red powder, m.p. 185°C. - ¹H NMR (CDCl₃): δ 8.48 (d, ³J_{HH} = 5.3 Hz, 4H, H-α, C₅H₄N), 7.23 (d, ³J_{HH} = 5.3 Hz, 4H, H-β, C₅H₄N), 4.60 (t, ^[68] ³J_{HH} = 1.88 Hz, 4H, H-α, C₅H₄), 4.37 (t, ^[69] ³J_{HH} = 1.88 Hz, 4H, H-β in C₅H₄); - ¹³C{¹H} NMR: 149.75 (C-2, C-6, C₅H₄N), 131.96 (C-4, C₅H₄N), 125.43 (C-3, C-5, C₅H₄N), 92.53, 84.73 (C≡C), 73.50, 71.56 (C₄H₄C), 66.09 (C₄H₄C). - MS (EI); *m/z*: 387.9 (M⁺). - IR (KBr, cm⁻¹): ν = 2205 s (C≡C), 1595 s (C=N). - C₂₄H₁₆FeN₂ · 0.05 CH₂Cl₂ (392.50): calcd. C 73.60, H 4.13, N 7.14; found C 73.87, H 3.86, N 6.99.

3.2.1.2 1,1'-Bis(3-pyridylethynyl)ferrocene (**1b**)

Yield (144 mg, 37%), air stable, red crystals, m.p. 195°C. - ¹H NMR (CD₂Cl₂): δ = 8.50 (dd, ⁴J_{HH} = 2.20, ⁵J_{HH} = 0.82 Hz, 4H, H-2, C₅H₄N), 8.35 (dd, ³J_{HH} = 4.87, ⁴J_{HH} = 1.73 Hz, 4H, H-6, C₅H₄N), 7.63 (ddd, ³J_{HH} = 7.91, ⁴J_{HH} = 1.92, ⁴J_{HH} = 1.92 Hz, 4H, H-4, C₅H₄N), 7.05 (ddd, ³J_{HH} = 7.91, ⁴J_{HH} = 4.87, ⁵J_{HH} = 0.82 Hz, 4H, H-5, C₅H₄N), 4.50 (m, ^[68] 8H, C₄H₄C), 4.29 (m, ^[69] 8H, C₄H₄C). - ¹³C{¹H} NMR (CD₂Cl₂): δ = 152.17 (C-2), 148.23 (C-6), 138.11 (C-4), 123.24 (C-5),

121.10 (C-3), 90.55, 83.79 (C≡C), 73.38, 71.41 (C₄H₄C), 66.96 (C₄H₄C). - MS (EI); *m/z*: 388.0 [M⁺]. - IR (KBr, cm⁻¹): ν = 2206 s (C≡C), 1595 w (C=N). - C₂₄H₁₆FeN₂ · 0.05 CH₂Cl₂ (392.50): calcd. C 73.60, H 4.13, N 7.14; found C 73.44, H 4.18, N 6.98.

3.2.1.3 1,1'-Bis(2,2'-bipyridine-5-ylethynyl)ferrocene (**1c**)

Yield (105 mg, 19%), air stable, red powder, m.p. >260°C (dec.). - ¹H NMR (CD₂Cl₂): δ = 8.53 (d, ⁴*J*_{HH} = 2.1 Hz, 2H, H-6), 8.50 (ddd, ³*J*_{HH} = 4.8, ⁴*J*_{HH} = 1.7, ⁵*J*_{HH} = 0.7 Hz, 2H, H-6'), 8.20 (ddd, ³*J*_{HH} = 8.0, ⁴*J*_{HH} = 1.0, ⁵*J*_{HH} = 1.0 Hz, 2H, H-3'), 8.18 (d, ³*J*_{HH} = 8.2 Hz, 2H, H-3), 7.69 (dd, ³*J*_{HH} = 8.2, ⁴*J*_{HH} = 2.1 Hz, 2H, H-4), 7.55 (ddd, ³*J*_{HH} = 7.7, ³*J*_{HH} = 7.7, ⁴*J*_{HH} = 1.7 Hz, 2H, H-4'), 7.12 (ddd, ³*J*_{HH} = 7.5, ⁴*J*_{HH} = 4.8, ⁵*J*_{HH} = 1.2 Hz, 2H, H-5'), 4.62 (m, ^[68] 4H, C₄H₄C), 4.40 (m, ^[69] 4H, C₄H₄C). - MS (EI); *m/z*: 542.0 [M⁺]. - IR (KBr, cm⁻¹): ν = 2207 s (C≡C). - C₃₄H₂₂FeN₄ · 0.1 CH₂Cl₂ (550.91): calcd. C 74.34, H 4.06, N 10.17; found C 73.99, H 3.83, N 10.18.

3.2.2 1,1'-Bis{[2,5-dipropoxy-4-(triisopropylsilylethynyl)phenyl]ethynyl}ferrocene (**8**)

To a solution of 1,1'-diiodoferrocene (642 mg, 1.47 mmol) and 1-ethynyl-4-(triisopropylsilyl)ethynyl-2,5-dipropoxybenzene (1245 mg, 3.1 mmol) in a mixture of triethylamine/diisopropylamine (50/20 mL) Pd(PPh₃)₂Cl₂ (102 mg, 0.15 mmol) and CuI (108 mg, 0.57 mmol) were added. The mixture was refluxed at 80°C for 2 d followed by removal of the solvents under vacuum. The residue was extracted with diethyl ether (4 × 100 mL) and the organic layer was dried over magnesium sulfate. After removal of the solvent by a rotation evaporator, the residue was subjected to column chromatography (aluminum oxide, 0-5% diethyl ether in *n*-hexane). The desired ferrocene derivative **8** was isolated in the third fraction. Yield (798 mg, 55%), orange, air-stable powder, m.p. 149°C. - ¹H NMR (CDCl₃): δ = 6.92 (s, 2H, C₆H₂), 6.88 (s, 2H, C₆H₂), 4.57 (m, ^[68] 4H, C₄H₄C), 4.35 (m, ^[69] 4H, C₄H₄C), 3.96 (t, ³*J*_{HH} = 6.4 Hz, 4H, OCH₂CH₂CH₃), 3.85 (t, ³*J*_{HH} = 6.4 Hz, 4H, OCH₂CH₂CH₃), 1.85 (m, 8H, OCH₂CH₂CH₃), 1.15 (s, 42H, SiC₉H₂₁), 1.03 (m, 12H, OCH₂CH₂CH₃). - ¹³C{¹H} NMR (CDCl₃): δ = 154.29, 153.15 (C-2 and C-5, C₆H₂), 117.52, 116.19 (C-3 and C-6, C₆H₂), 114.59, 113.35 (C-1 and C-4, C₆H₂), 103.06,

96.00(C≡C-SiC₉H₂₁), 92.87, 82.69 (C≡C-C₅H₄), 73.00 (C₄H₄C), 71.44(C₄H₄C), 71.05, 70.60 (OCH₂CH₂CH₃), 66.64 (C₄H₄C), 22.74, 22.61 (OCH₂CH₂CH₃), 18.64, 11.30 (SiC₉H₂₁), 10.62, 10.57 (OCH₂CH₂CH₃). - MS (EI); *m/z*: 978.5 [M⁺]. - IR (KBr, cm⁻¹): ν = 2150 s (C≡C). - C₆₀H₈₂FeO₄Si₂ (979.32): calcd. C 73.59, H 8.44; found C 73.50, H 7.94.

3.2.3 General Procedure for the Preparation of Ligands **10a-d**

To a solution of **8** (980 mg, 1.0 mmol) in THF (50 mL) two equivalents of tetra-*n*-butylammonium fluoride (520 mg, 2.0 mmol) were added at 20°C. The solution was stirred for 2 h at the same temperature. Then a 50% excess of 4-bromopyridine hydrochloride, 5-bromo-2,2'-bipyridine, and 3-bromo-1,10-phenanthroline, respectively, diisopropylamine (20 mL) (and in the case of phenanthroline also 20 mL of *n*-propylamine) as well as Pd(PPh₃)Cl₂ (35 mg, 0.05 mmol) and CuI (20 mg, 0.1 mmol) were added. In the case of phenanthroline additional Pd(PPh₃)₄ was used as a catalyst. The oil-bath temperature was controlled at 80°C, and the mixture was stirred for 2 d. After cooling down to room temperature, the solvents were removed under vacuum and a concentrated aqueous ammonium chloride solution (50 mL) was added. The residue was extracted at least four times, each with 50 mL of dichloromethane. The organic extract was washed with 200 mL of an aqueous sodium chloride solution and finally it was dried over magnesium sulfate. After removal of the solvents, the residue was ready for column chromatography using silica gel and dichloromethane. The product was eluted by a solvent mixture of methanol (0-5%), THF (10-50%), and dichloromethane. Recrystallization from dichloromethane and *n*-pentane gave spectroscopically pure products.

3.2.3.1 1,1'-Bis{[4-(4-pyridylethynyl)-2,5-dipropoxyphenyl]ethynyl} ferrocene (**10a**)

Yield (427 mg, 52%), orange powder, m.p. 161°C. - ¹H NMR (CDCl₃): δ = 8.50 (d, ³*J*_{HH} = 5.0 Hz, 4H, H- α , C₅H₄N), 7.34 (d, ³*J*_{HH} = 5.0 Hz, 4H, H- β , C₅H₄N), 6.96 (s, 2H, C₆H₂), 6.91(s, 2H, C₆H₂), 4.57 (m,^[68] 4H, C₄H₄C), 4.36 (m,^[69] 4H, C₄H₄C), 3.95 (t, ³*J*_{HH} = 6.1 Hz, 4H, OCH₂CH₂CH₃), 3.91 (t, ³*J*_{HH} = 6.4 Hz, 4H, OCH₂CH₂CH₃), 1.86 (m, 8H, OCH₂CH₂CH₃), 1.10 (m,

12H, OCH₂CH₂CH₃). - ¹³C{¹H} NMR (CDCl₃): δ = 153.90, 153.28 (C-2 and C-5, C₆H₂), 149.66 (C-α, C₅H₄N), 131.57 (C-γ, C₅H₄N), 125.27 (C-β, C₅H₄N), 116.81, 116.50 (C-3 and C-6, C₆H₂), 115.74, 111.70 (C-1 and C-4, C₆H₂), 93.58, 91.60, 90.77, 82.61 (C≡C-C₆H₂-C≡C), 72.93 (C₄H₄C), 71.50 (C₄H₄C), 70.94, 70.79 (OCH₂CH₂CH₃), 66.62 (C₄H₄C), 22.67, 22.62 (OCH₂CH₂CH₃), 10.60, 10.50 (OCH₂CH₂CH₃). - MS (FD); *m/z*: 820.6 [M⁺]. - IR (KBr, cm⁻¹): ν = 2213 s (C≡C). - C₅₂H₄₈FeN₂O₄ (820.80): calcd. C 76.09, H 5.89, N 3.41; found C 75.85, H 5.41, N 3.28.

3.2.3.2 1,1'-Bis{[4-(3-pyridylethynyl)-2,5-dipropoxyphenyl]ethynyl}ferrocene (**10b**)

Yield (399 mg, 48%), orange powder, m.p. 155°C. - ¹H NMR (CD₂Cl₂): δ = 8.72 (d, ³J_{HH} = 2.2 Hz, 2H, H-2, C₅H₄N), 8.51 (dd, ³J_{HH} = 4.9, ⁴J_{HH} = 1.6 Hz, 2H, H-6, C₅H₄N), 7.78 (ddd, ³J_{HH} = 7.8, ⁴J_{HH} = 1.8 Hz, ⁴J_{HH} = 1.8 Hz, 2H, H-4, C₅H₄N), 7.27 (dd, ³J_{HH} = 7.8, ³J_{HH} = 4.9 Hz, 2H, H-5, C₅H₄N), 6.99 (s, 2H, C₆H₂), 6.91 (s, 2H, C₆H₂), 4.58 (m, ^[68] 4H, C₄H₄C), 4.39 (m, ^[69] 4H, C₄H₄C), 3.96 (t, ³J_{HH} = 6.1 Hz, 4H, OCH₂CH₂CH₃), 3.91 (t, ³J_{HH} = 6.4 Hz, 4H, OCH₂CH₂CH₃), 1.86 (m, 8H, OCH₂CH₂CH₃), 1.11 (m, 12H, OCH₂CH₂CH₃). - ¹³C{¹H} NMR (CDCl₃): δ = 154.08, 153.71 (C-2 and C-5, C₆H₂), 152.34 (C-2, C₅H₄N), 148.85 (C-6, C₅H₄N), 138.41 (C-4, C₅H₄N), 123.41 (C-5, C₅H₄N), 120.89 (C-3, C₅H₄N), 117.10, 116.83 (C-3 and C-6, C₆H₂), 115.52, 112.65 (C-1 and C-4, C₆H₂), 93.42, 91.30, 89.58, 83.21 (C≡C-C₆H₂-C≡C), 73.32 (C₄H₄C), 71.74 (C₄H₄C), 71.36, 71.23 (OCH₂CH₂CH₃), 67.30 (C₄H₄C), 23.10, 23.07 (OCH₂CH₂CH₃), 10.79, 10.71 (OCH₂CH₂CH₃). - MS (FD); *m/z*: 820.6 [M⁺]. - IR (KBr, cm⁻¹): ν = 2214 w (C≡C). - C₅₂H₄₈FeN₂O₄ (820.80): calcd. C 76.09, H 5.89, N 3.41; found C 75.78, H 5.39, N 3.38.

3.2.3.3 1,1'-Bis{[4-(2,2'-bipyridine-5-ylethynyl)-2,5-dipropoxy-phenyl]ethynyl}ferrocene (**10c**)

Yield (440 mg, 45%), orange powder, m.p. 165°C. - ¹H NMR (CDCl₃): δ = 8.80 (dd, ⁴J_{HH} = 2.2, ⁵J_{HH} = 0.8 Hz, 2H, H-6), 8.67 (ddd, ³J_{HH} = 4.7, ⁴J_{HH} = 1.7, ⁵J_{HH} = 0.9 Hz 2H, H-6'), 8.40 (ddd, ³J_{HH} = 8.0, ⁴J_{HH} = 1.0, ⁵J_{HH} = 1.0 Hz 2H, H-3'), 8.37 (dd, ³J_{HH} = 8.2, ⁵J_{HH} = 0.8 Hz, 2H, H-3), 7.92 (dd, ³J_{HH} = 8.2, ⁴J_{HH} = 2.2 Hz, 2H, H-4), 7.80 (ddd, ³J_{HH} = 7.8, ³J_{HH} = 7.8, ⁴J_{HH} = 1.7 Hz, 2H, H-4'), 7.30 (ddd, ³J_{HH} = 7.5, ³J_{HH} = 4.8, ⁴J_{HH} = 1.1 Hz, 2H, H-5' in C₁₀H₇N₂), 6.99 (s, 2H, C₆H₂),

6.93 (s, 2H, C₆H₂), 4.59 (m,^[68] 4H, C₄H₄C), 4.37 (m,^[69] 4H, C₄H₄C); 3.99 (t, ³J_{HH} = 6.44 Hz, 4H, OCH₂CH₂CH₃), 3.94 (t, ³J_{HH} = 6.44 Hz, 4H, OCH₂CH₂CH₃), 1.88 (m, 8H, OCH₂CH₂CH₃), 1.13 (t, ³J_{HH} = 7.38 Hz, 6H, OCH₂CH₂CH₃), 1.11 (t, ³J_{HH} = 7.38 Hz, 6H, OCH₂CH₂CH₃). - ¹³C{¹H} NMR (CDCl₃): δ = 155.43, 154.57 (C-2 and C-2', C₁₀H₇N₂), 153.73, 153.38 (C-2 and C-5, C₆H₂), 151.52, 149.22 (C-6 and C-6', C₁₀H₇N₂), 139.09, 136.90 (C-4 and C-4', C₁₀H₇N₂), 123.82, 121.26 (C-3 and C-3', C₁₀H₇N₂), 120.58 (C-5, C₁₀H₇N₂), 120.30 (C-5', C₁₀H₇N₂), 116.70, 116.59 (C-3 and C-6, C₆H₂), 115.23, 112.40 (C-1 and C-4, C₆H₂), 93.33, 91.47, 90.35, 82.76 (C≡C-C₆H₂-C≡C), 72.93, 71.52 (C₄H₄C), 70.99, 70.90 (OCH₂CH₂CH₃), 66.77 (C₄H₄C), 22.74 (OCH₂CH₂CH₃), 10.67, 10.59 (OCH₂CH₂CH₃). - MS (EI); *m/z*: 974.3(M⁺). IR (KBr, cm⁻¹): ν = 2216 s (C≡C). - C₆₂H₅₄FeN₄O₄ (974.98): calcd. C 76.38, H 5.58, N 5.75; found C 76.01, H 5.94, N 5.20.

3.2.3.4 1,1'-Bis{[4-(1,10-phenanthroline-3-ylethynyl)-2,5-dipropoxy-phenyl]ethynyl}ferrocene (**10d**)

Initial weights: 3-bromo-1,10-phenanthroline (780 mg, 3.0 mmol), Pd(PPh₃)₄ (140 mg, 0.12 mmol), Pd(PPh₃)₂Cl₂ (14 mg, 0.02 mmol), and CuI (15 mg, 0.08 mmol). Prior to chromatography the copper complex was extracted with a 2% solution of KCN in water (100 mL). Recrystallization was carried out with chloroform and *n*-hexane. Yield (521 mg, 51%), orange powder, m.p. 172°C. - ¹H NMR (CD₂Cl₂): δ = 9.13 (d, ⁴J_{HH} = 2.0 Hz, 2H, H-2, C₁₂H₇N₂), 9.04 (dd, ³J_{HH} = 4.3, ⁴J_{HH} = 1.7 Hz, 2H, H-9, C₁₂H₇N₂), 8.10 (d, ⁴J_{HH} = 2.0 Hz, 2H, H-4, C₁₂H₇N₂), 8.01 (dd, ³J_{HH} = 8.0, ⁴J_{HH} = 1.7 Hz, 2H, H-7, C₁₂H₇N₂), 7.53 (dd, ³J_{HH} = 8.0, ³J_{HH} = 4.3 Hz, 2H, H-8, C₁₂H₇N₂), 7.47 (s, 4H, H-5 and H-6, C₁₂H₇N₂), 6.96 (s, 2H, H-3 or 6, C₆H₂), 6.81 (s, 2H, H-3 or 6, C₆H₂), 4.58 (m,^[68] 4H, C₄H₄C), 4.38 (m,^[69] 4H, C₄H₄C), 3.96 (t, ³J_{HH} = 6.4 Hz, 4H, OCH₂CH₂CH₃), 3.93 (t, ³J_{HH} = 6.4 Hz, 4H, OCH₂CH₂CH₃), 1.91 (m, 8H, OCH₂CH₂CH₃), 1.19 (t, ³J_{HH} = 7.4 Hz, 6H, OCH₂CH₂CH₃), 1.15 (t, ³J_{HH} = 7.5 Hz, 6H, OCH₂CH₂CH₃). - ¹³C{¹H} NMR(CD₂Cl₂): δ = 154.05, 153.44 (C-2 and C-5 in C₆H₂), 151.85 (C-2), 150.38 (C-9), 145.93 (C-1a), 144.48 (C-10a), 137.44 (C-4), 135.92 (C-7), 128.94 (C-6a), 127.80 (C-4a), 127.16, 126.07 (C-

5 and C-6), 123.12 (C-8), 119.96 (C-3, C₁₂H₇N₂), 116.97, 116.38 (C-3 and C-6, C₆H₂), 115.68, 112.37, (C-1 and C-4, C₆H₂), 92.73, 91.72, 90.87, 83.89 (C≡C-C₆H₂-C≡C), 72.91 (C₄H₄C), 71.24 (OCH₂CH₂CH₃), 71.05 (C₄H₄C), 71.02 (OCH₂CH₂CH₃), 68.18 (C₄H₄C), 23.10 (OCH₂CH₂CH₃), 23.07 (OCH₂CH₂CH₃), 10.77 (OCH₂CH₂CH₃), 10.75 (OCH₂CH₂CH₃). - MS (FAB); *m/z*: 1023.1(M⁺). - IR (KBr, cm⁻¹): $\nu = 2202$ s (C≡C). - C₆₆H₅₄FeN₄O₄ · 0.5 CHCl₃ (1082.71): calcd. C 73.72, H 5.07, N 5.18; found C 73.46, H 5.45, N 5.19.

3.2.4 Preparation of Macrocycles **11a,b** and **12b**

3.2.4.1 Heterotetranuclear Fe₂Ni₂ Complex **11a**

Solutions of nickel(II) nitrate hexahydrate (74 mg, 0.25 mmol) in methanol (50 mL) and of ligand **1** (98 mg, 0.25 mmol) in dichloromethane (50 mL) were simultaneously added dropwise to a stirred mixture of dichloromethane and methanol (50/50 mL) within 4 h at room temperature. The resulting red mixture was stirred for 20 h at the same temperature. Then the solvents were removed under vacuum. The red residue was washed with methanol (2 mL) and dichloromethane (5 mL) and dried in vacuo for 15 h. Yield 136 mg (92%), red solid, m.p. > 270°C. - FT-IR (KBr, cm⁻¹): $\nu = 2207$ s (C≡C), 1611 vs (C=N), 1289 s (NO₃⁻), 1218 sh (NO₃⁻). - C₄₈H₃₂Fe₂N₈Ni₂O₁₂ · 0.5 CH₂Cl₂ (1184.37): calcd. C 49.18, H 2.81, N 9.46; found C, 49.12 H, 2.88 N 9.25.

3.2.4.2 Heterotetranuclear Fe₂Ag₂ Complex **11b**

Solutions of ligand **1b** (42 mg, 0.108 mmol) in a mixture of acetonitrile/dichloromethane (25/2 mL) and of silver(I) perchlorate (23.5 mg, 0.114 mmol) in acetonitrile (20 mL) were simultaneously added dropwise to stirred dichloromethane (20 mL) at room temperature during a period of 2 h. After the addition, the mixture was stirred for 24 h at the same temperature followed by the removal of solvents under vacuum. The precipitate was filtered (P3) and washed with dichloromethane (3 mL) and finally dried in vacuo. Warning! This perchlorate complex is hazardous because of the possibility of explosion. *It is worthy of noting that compound 11b*

exploded at about 220°C during the measurement of the melting point. Special care should be given and only very small amounts of the sample should be handled. Yield 64.5 mg (94%), red powder, m.p. >220°C (explosive). ¹H NMR (CD₃CN): δ = 8.49 (dd, ⁴J_{HH} = 2.20, ⁵J_{HH} = 0.71 Hz, 4H, H-2, C₅H₄N), 8.41 (dd, ³J_{HH} = 4.94, ⁴J_{HH} = 1.57 Hz, 4H, H-6, C₅H₄N), 7.64 (ddd, ³J_{HH} = 7.98, ⁴J_{HH} = 1.88, ⁴J_{HH} = 1.88 Hz, 4H, H-4, C₅H₄N), 7.20 (ddd, ³J_{HH} = 7.98, ⁴J_{HH} = 4.94, ⁵J_{HH} = 0.71 Hz, 4H, H-5, C₅H₄N), 4.50 (m, ^[68] 8H, C₄H₄C), 4.29 (m, ^[69] 8H, C₄H₄C). - IR (KBr, cm⁻¹): ν = 2211 m (C≡C), 1593 w (C=N), 1095 vs, 1050 s (ClO₄⁻). - C₄₈H₃₂Ag₂Cl₂Fe₂N₄O₈ · CH₃CN · 0.5 CH₂Cl₂ (1274.66): calcd. C 47.59, H 2.85, N 5.49; found C 47.30, H 2.83, N 5.30.

3.2.4.3 Heterotetranuclear Fe₂Pd₂ Complex **12b**

Solutions of ligand **1b** (77 mg, 0.2 mmol) in dichloromethane (50 mL) and of PdCl₂(COD) (57 mg, 0.2 mmol) in dichloromethane (50 mL) were simultaneously added dropwise to stirred dichloromethane (50 mL) at room temperature during a period of 1 h. After the addition, the mixture was stirred for 20 h at the same temperature followed by the removal of solvents under vacuum. The precipitate was filtered and washed with dichloromethane (3 mL) and finally dried in vacuo. Yield 107 mg (95%), red powder, m.p. >270°C. ¹H NMR (CD₂Cl₂): δ = 8.68 (d, ⁴J_{HH} = 2.51 Hz, 4H, H-2, C₅H₄N), 8.66 (dd, ³J_{HH} = 6.08, ⁴J_{HH} = 1.30 Hz, 4H, H-6, C₅H₄N), 7.36 (ddd, ³J_{HH} = 7.96, ⁴J_{HH} = 1.90, ⁴J_{HH} = 1.90 Hz, 4H, H-4, C₅H₄N), 6.74 (ddd, ³J_{HH} = 7.96, ⁴J_{HH} = 6.08, ⁵J_{HH} = 0.67 Hz, 4H, H-5, C₅H₄N), 4.55 (m, ^[68] 8H, C₄H₄C), 4.30 (m, ^[69] 8H, C₄H₄C). - IR (KBr, cm⁻¹): ν = 2209 s (C≡C), 1596 w (C=N), 1095 vs, 1050 s (ClO₄⁻). - C₄₈H₃₂Cl₄Fe₂N₄Pd₂ (1131.15): calcd. C 50.97, H 2.85, N 4.95, Cl 12.54; found C 50.58, H 2.68, N 4.83, Cl 12.57.

3.2.5 General Procedure for the Preparation of the Bimetallic Complexes

Solutions of a ligand (**10c** or **10d**, 0.08 mmol) in chloroform or dichloromethane (25 mL) and of an equal mole of transition metal salt in methanol (zinc(II) acetate, silver(I) triflate,) or acetonitrile (iron(II) perchlorate) were mixed dropwise at room temperature. After 1 d stirring at

the same temperature, solvents were removed. The residue was purified by recrystallization from dichloromethane and diethyl ether, and intensively washed with *n*-pentane.

3.2.5.1 Zn(CH₃COO)₂ · **10c** (**13c**)

Yield 80.0%, red powder, m.p. >250 °C, dec. - ¹H NMR (CDCl₃): δ = 8.87 (4H, bipy), 7.99 (2H, bipy), 7.85 (4H, bipy), 7.68 (2H, bipy), 7.40 (2H, bipy), 6.76 (4H, C₆H₂), 6.62 (2H, C₆H₂), 4.55 (4H, C₅H₄), 4.33 (4H, C₅H₄), 3.88 (m, 8H, OCH₂CH₂CH₃), 2.14 (6H, CH₃COO⁻), 1.90 (m, 8H, OCH₂CH₂CH₃), 1.15 (m, 12H, OCH₂CH₂CH₃). - MS (FAB); *m/z*: 1099.2 [M-Ac+2H]⁺, 1038.9 [M-2Ac]⁺. - IR (KBr, cm⁻¹): ν = 2215 w (C≡C), 1730 vs, (C=O), 1600 s (C=N). - C₆₆H₆₀FeN₄O₈Zn · 2 CHCl₃ (1397.19): calcd. C 58.45, H 4.47, N 4.01; found C 58.15, H 4.72, N 3.85.

3.2.5.2 Zn(CH₃CO₂)₂ · **10d** (**13d**)

Yield 75%, red powder, m.p. >250 °C, dec. - ¹H NMR (CDCl₃): δ = 9.25 (4H, phen), 8.22 (2H, phen), 8.08 (2H, phen), 7.80 (2H, phen), 7.70 (2H, phen), 7.46 (2H, phen), 6.88 (s, 2H, C₆H₂), 6.76 (s, 2H, C₆H₂), 4.58 (4H, C₅H₄), 4.35 (4H, C₅H₄), 3.95 (m, 8H, OCH₂CH₂CH₃), 2.14 (6H, CH₃COO⁻), 1.94 (m, 8H, OCH₂CH₂CH₃), 1.18 (m, 12H, OCH₂CH₂CH₃). - MS (FAB); *m/z*: 1145.2 ([M-CH₃COO]⁺), 1087.2([M-2CH₃COO+H]⁺); - IR (KBr, cm⁻¹): ν = 2203 m (C≡C), 1725 w (C=O). - C₇₀H₆₀FeN₄O₈Zn · 2.5 CH₂Cl₂ (1418.83): C 61.37, H 4.62, N 3.95; found C 61.71, H 4.37, N 3.91.

3.2.5.3 Ag(CF₃SO₃) · **10d** (**14d**)

Yield 85%, red powder, m.p. >250 °C, dec. - ¹H NMR (CD₃CN): δ = 8.83 (2H, H-2, phen), 8.56 (2H, H-9, phen), 8.03 (2H, H-4, phen), 7.79 (2H, H-7, phen), 7.58 (2H, H-8, phen), 7.33 (2H, H-5 or H-6, phen), 7.23 (2H, H-6 or H-5, phen), 6.14 (2H, C₆H₂), 6.08 (2H, C₆H₂), 4.42 (4H, C₅H₄), 4.34 (4H, C₅H₄), 3.04 (8H, OCH₂CH₂CH₃), 1.58 (8H, OCH₂CH₂CH₃), 0.93 (12H, OCH₂CH₂CH₃). -MS (FAB); *m/z*: 1131.3 ([M-CF₃SO₃]⁺). - IR (KBr, cm⁻¹): ν = 2201 m (C≡C). -

$C_{67}H_{54}AgF_3FeN_4O_7S \cdot 0.5 CH_2Cl_2$ (1322.42): calcd. C 61.31, H 4.19, N 4.24, S 2.42; found C 61.35, H 4.53, N 4.14, S 2.21.

3.2.5.4 $Fe(ClO_4)_2 \cdot \mathbf{10d}$ (**15d**)

Yield 95%, dark red solid, m.p. > 250°C, dec. - 1H NMR (CD_3CN): δ = 8.66 (4H, H-2, H-9), 8.30 (4H, H-4, H-7), 7.65 (6H, H-6, H-5, H-8), 6.97 (4H, C_6H_2) 4.40 (4H, C_5H_4), 3.86 (4H, C_5H_4), 3.67(8H, $OCH_2CH_2CH_3$), 1.67(8H, $OCH_2CH_2CH_3$), 0.91(12H, $OCH_2CH_2CH_3$). - MS (FAB); m/z : 1177.4 ($[M-ClO_4]^+$) and 1078.5 ($[M-2ClO_4]^+$). - IR (KBr, cm^{-1}): ν = 2201 s ($C\equiv C$), 1597 sh ($C=N$), 1583 s, ($C=N$), 1211 s, 1095 vs ($Cl-O$); - $C_{66}H_{54}Cl_2Fe_2N_4O_{12} \cdot 5 H_2O$ (1367.84): calcd. C 57.95, H 4.71, N 4.10; found C 57.50, H 4.57, N 4.12.

3.3 X-ray Crystallographic Studies

Crystallographic and data collection information as well as a description of the structural analyses and refinements for ligands **1a,b** and complexes **11a**, **11b**, and **12b** are summarized in Table 5. Single crystals of **1a** and **1b** were obtained by slow evaporation of their solutions in dichloromethane-methanol. Single crystals of **11a** of X-ray quality were obtained by slow diffusion of ligand **1a** in dichloromethane into a solution of nickel(II) nitrate hexahydrate in methanol.^[70] Suitable single crystals of **11b** were obtained by slow diffusion of ligand **1b** in dichloromethane into a solution of silver(I) perchlorate in acetonitrile. Crystals of **12b** were obtained by slow diffusion of a $PdCl_2(COD)$ solution in dichloromethane into a dichloromethane solution of ligand **1b** at room temperature. Each crystal was fixed on a glass fiber using perfluoropolyether RS 3000 and transferred to a Siemens P4 diffractometer (**1b**, **11a,b**) or a Stoe IPDS diffractometer (**1a**, **12b**) using graphite-monochromated $Mo-K_\alpha$ radiation. The lattice constants for ligand **1b** and macrocycles **11a** and **11b** were determined by 50 precisely centered high-angle reflections. Intensities were collected by the ω -scan technique. Empirical absorption correction was made in each case. The structures were solved by direct methods with SHELXTL

V5.1 (NT version)^[71] (**1b**, **11a**, and **11b**) and SHELXS^[72] (**1a** and **12b**), and refined by least squares using the same program (**1b**, **11a**, and **11b**) and SHELXL 97^[73] with anisotropic thermal parameters for all non-hydrogen atoms. All hydrogen atoms were located in calculated positions (riding mode), with the exception of the hydrogen atoms of the water molecule in **1a**, which were located in the difference electron density map and refined isotropically. The largest peak and hole in the last difference synthesis were 0.980/-0.373 (**1a**), 0.120/-0.252 (**1b**), 1.175/-0.696 (**11a**), 0.520/-0.500 (**11b**), and 2.823/-2.497 (**12b**) e Å⁻³, respectively. CCDC-185968 (**1a**), CCDC-190120 (**11a**), and CCDC-190121 (**11b**) contain the supplementary crystallographic data for this work. These data can be obtained free of charge at www.ccdc.cam.ac.uk/conts/retrieving.html [or from the Cambridge Crystallographic Data Center, 12, Union Road, Cambridge CB2 1EZ, UK; fax: (internat.) +44-1223/336-033; E-mail: deposit@ccdc.cam.ac.uk].

3.4 Electrochemical Experiments

All electrochemical experiments were performed with a Bioanalytical CV-50W Voltammetric Analyzer (BAS, West Lafayette, IN, USA) controlled by a standard 80486 personal computer (control program version 2.0). For electroanalytical experiments a Metrohm platinum tip electrode (Filderstadt, Germany) was applied as working electrode. The counter electrode was a platinum wire of 1 mm in diameter. A single-unit Haber-Luggin Ag⁺/Ag double reference electrode was used. The resulting potential values refer to Ag/Ag⁺ (0.01 M in CH₃CN/0.1 M NBu₄PF₆). Ferrocene was used as an external standard. Its potentials of 102.5 mV (in CH₃CN) and 214.5 mV (in CH₂Cl₂) were determined by separate cyclic voltammetric experiments in the respective solvent, and all potentials here are reported relative to the fc/fc⁺ standard. For cyclic voltammetry, a glass-tight full-glass three-electrode cell was used and its assembly for the experiments has been described.^[74] The cell was purged with argon before it was filled with the electrolyte. Background curves were recorded before adding the substrate to the solution. These

were later subtracted from the experimental data of the samples (excluding complex **11a**). The automatic BAS CV-50W *iR*-drop compensation facility was used for all experiments.

3.5 Magnetic Experiment

Magnetic susceptibility of a powdered sample packed in a capsule was measured using a SQUID Quantum Design MPMS magnetometer at 10000 Gauss over the temperature range 5 - 300 K. All data were corrected for sample holder contribution. Diamagnetism of the sample and paramagnetism of nickel(II) were represented by a parameter in the non-linear fit equation. This parameter was found to be $(5.4 \pm 1.4) \times 10^{-4}$ emu/mol.

Table 1. Atomic coordinates ($\times 10^4$) and equivalent isotropic displacement parameters ($\text{Å}^2 \times 10^3$) for **1a** U(eq) is defined as one third of the trace of the orthogonalized Uij tensor

Atom	x	y	z	U(eq)
Fe(1)	-225(2)	6765(1)	7796(1)	47(1)
Fe(2)	6022(2)	3761(1)	2790(1)	53(1)
C(1)	21(11)	5750(9)	8669(11)	42(3)
C(2)	145(12)	5322(9)	7688(10)	44(3)
C(3)	-1023(13)	5114(10)	6879(11)	57(4)
C(4)	-1870(15)	5433(12)	7359(14)	53(4)
C(5)	-1281(13)	5842(12)	8444(15)	46(5)
C(6)	1001(11)	6094(9)	9688(10)	40(3)
C(7)	1853(11)	6368(9)	10488(10)	38(3)
C(8)	2869(13)	6705(11)	11500(13)	38(4)
C(9)	4052(10)	6514(9)	11587(9)	46(3)
C(10)	4972(11)	6836(9)	12556(10)	52(3)
N(1)	4901(9)	7364(8)	13474(9)	60(3)
C(11)	3787(13)	7542(10)	13386(10)	56(4)
C(12)	2748(13)	7421(10)	12471(12)	45(4)
C(13)	1110(12)	8356(10)	8603(13)	53(4)
C(14)	1220(14)	7903(9)	7627(11)	50(4)
C(15)	27(16)	7638(11)	6817(13)	72(5)
C(16)	-856(15)	7921(12)	7319(15)	67(5)
C(17)	-182(14)	8364(11)	8407(15)	63(5)
C(18)	2086(12)	8754(9)	9612(12)	48(4)
C(19)	2906(12)	9099(10)	10456(11)	46(3)
C(20)	3859(16)	9527(11)	11483(14)	50(4)
C(21)	5126(14)	9471(10)	11685(13)	73(4)
C(22)	6004(15)	9942(13)	12732(18)	92(6)
N(2)	5748(16)	10444(11)	13555(12)	92(5)
C(23)	4542(16)	10496(11)	13357(13)	81(5)
C(24)	3595(14)	10050(10)	12379(13)	64(4)
C(25)	5709(11)	4058(9)	1391(9)	45(3)
C(26)	4562(11)	3837(9)	1638(9)	53(3)
C(27)	4207(12)	2767(10)	1707(10)	66(4)
C(28)	5199(15)	2324(13)	1477(13)	59(5)
C(29)	6097(12)	3103(9)	1310(10)	48(3)
C(30)	6445(12)	5059(11)	1287(10)	38(3)
C(31)	7044(12)	5879(10)	1180(10)	39(3)
C(32)	7813(11)	6865(9)	1088(8)	40(3)
C(33)	7288(12)	7685(9)	957(10)	54(4)
C(34)	8089(18)	8611(12)	838(12)	72(5)
N(3)	9292(13)	8803(9)	893(10)	70(3)
C(35)	9770(12)	8031(9)	1051(9)	56(3)
C(36)	9102(11)	7083(9)	1158(9)	49(3)
C(37)	7432(12)	5098(10)	4013(9)	49(3)
C(38)	6211(14)	4892(10)	4165(10)	65(4)
C(39)	5808(14)	3797(10)	4200(10)	71(4)
C(40)	6789(15)	3338(11)	4030(12)	63(5)

to be continued on next page

Table 1. Continuation

C(41)	7774(13)	4146(10)	3932(10)	50(3)
C(42)	8186(13)	6128(11)	3952(10)	42(3)
C(43)	8831(13)	6971(10)	3930(10)	45(3)
C(44)	9639(11)	8035(9)	3963(8)	39(3)
C(45)	9107(11)	8762(9)	3643(10)	51(4)
C(46)	9920(14)	9729(11)	3668(11)	56(4)
N(4)	11226(11)	10062(8)	4004(8)	64(3)
C(47)	11743(13)	9371(10)	4321(11)	70(4)
C(48)	11004(13)	8348(10)	4295(10)	60(3)
O(1)	6726(10)	7796(9)	5421(9)	84(4)

Table 2. Atomic coordinates ($\times 10^4$) and equivalent isotropic displacement parameters ($\text{Å}^2 \times 10^3$) for **1b** U(eq) is defined as one third of the trace of the orthogonalized U_{ij} tensor

Atom	x	y	z	U(eq)
Fe(1)	6691(1)	12367(1)	5981(1)	37(1)
C(1)	7670(5)	12695(9)	7551(9)	48(4)
C(2)	7773(6)	13481(11)	6507(10)	36(2)
C(3)	7105(7)	14375(9)	6117(9)	46(4)
C(4)	6589(5)	14141(8)	6920(9)	62(3)
C(5)	6939(4)	13103(8)	7806(7)	53(2)
C(6)	8311(7)	11739(12)	8212(13)	29(2)
C(7)	8709(11)	10853(16)	8834(11)	33(2)
C(8)	9200(8)	9780(14)	9419(12)	35(2)
C(9)	9789(6)	9226(9)	8861(8)	40(2)
C(10)	10296(6)	8223(12)	9494(9)	56(2)
C(11)	10203(6)	7786(8)	10670(8)	54(2)
N(1A)	9641(4)	8310(7)	11237(7)	58(2)
C(13)	9163(7)	9213(14)	10581(11)	47(3)
C(14)	6674(5)	11142(7)	4445(7)	45(2)
C(15)	6052(5)	12135(7)	4184(8)	75(5)
C(16)	5576(6)	11925(9)	5052(12)	64(5)
C(17)	5903(8)	10804(9)	5848(10)	52(3)
C(18)	6582(7)	10319(8)	5473(9)	43(5)
C(19)	7133(5)	9207(14)	6122(13)	42(4)
C(20)	7592(9)	8350(14)	6633(8)	44(4)
C(21)	8697(5)	6891(9)	6488(8)	44(2)
N(1B)	9248(4)	5944(7)	6915(6)	55(2)
C(23)	9247(6)	5370(10)	8028(9)	50(2)
C(24)	8690(9)	5706(10)	8740(9)	48(3)
C(25)	8121(9)	6703(18)	8249(15)	45(3)
C(26)	8108(7)	7313(13)	7083(12)	37(2)
Fe(1A)	9178(1)	7620(1)	8856(1)	38(1)
C(1A)	8936(7)	6915(9)	7009(9)	53(3)

to be continued on next page

Table 2. Continuation

C(2A)	9323(6)	5888(10)	7878(12)	56(3)
C(3A)	8846(9)	5628(15)	8734(13)	49(5)
C(4A)	8163(8)	6495(19)	8395(16)	32(4)
C(5A)	8218(7)	7291(15)	7329(13)	31(3)
C(6A)	7597(11)	8326(15)	6561(14)	37(5)
C(7A)	7161(10)	9243(14)	6060(20)	38(5)
C(8A)	6645(11)	10213(16)	5478(13)	35(5)
C(9A)	6060(16)	10770(20)	5934(17)	67(6)
C(10A)	5554(11)	11740(20)	5270(20)	63(5)
C(11A)	5684(9)	12156(16)	4118(12)	58(4)
N(1C)	6197(6)	11690(11)	3637(8)	57(2)
C(13A)	6713(7)	10673(10)	4288(13)	42(3)
C(14A)	9181(7)	8929(16)	10356(12)	57(6)
C(15A)	9822(6)	7983(119)	10762(9)	53(3)
C(16A)	10334(59)	8113(13)	9939(13)	56(4)
C(17A)	10010(6)	9139(16)	9024(11)	55(5)
C(18A)	9298(8)	9644(16)	9282(15)	31(4)
C(19A)	8158(10)	11494(18)	8818(19)	27(2)
C(20A)	8700(13)	10670(20)	8575(16)	25(2)
C(21A)	7731(7)	12626(13)	7628(14)	30(4)
C(22A)	7686(11)	13240(20)	6443(19)	42(4)
C(23A)	7132(16)	14230(20)	6044(18)	63(7)
C(24A)	6655(10)	14626(17)	6751(15)	61(4)
N(1D)	6636(6)	14081(89)	7865(10)	53(2)
C(26A)	7169(7)	13101(11)	8304(11)	40(2)

Table 3. Atomic coordinates ($\times 10^4$) and equivalent isotropic displacement parameters ($\text{Å}^2 \times 10^3$) for **11a** U(eq) is defined as one third of the trace of the orthogonalized Uij tensor

Atom	x	y	z	U(eq)
Ni	-1789(1)	5991(1)	9965(1)	24(1)
Fe	5467(1)	9263(1)	3131(1)	29(1)
O(1)	616(3)	5455(2)	10434(2)	32(1)
O(2)	327(3)	6803(2)	11029(2)	42(1)
O(3)	2645(3)	5552(2)	11139(2)	47(1)
O(4)	-3275(3)	7416(2)	10329(2)	38(1)
O(5)	-4215(3)	6608(2)	9531(2)	39(1)
O(6)	-5854(4)	8027(3)	9926(3)	75(1)
N(1)	-731(3)	6901(2)	8569(2)	27(1)
N(2)	2936(3)	4842(2)	8625(2)	24(1)
N(3)	-4506(3)	7378(2)	9936(2)	39(1)
N(4)	1221(3)	5953(2)	10886(2)	31(1)
C(1)	3063(4)	9790(2)	3921(2)	36(1)
C(2)	2924(4)	9675(3)	2954(2)	41(1)
C(3)	3904(5)	10366(3)	2166(2)	43(1)
C(4)	4671(4)	10894(2)	2621(2)	40(1)
C(5)	4171(4)	10541(2)	3710(2)	37(1)
C(6)	2269(4)	9224(2)	4905(2)	38(1)
C(7)	1559(4)	8739(2)	5712(2)	38(1)
C(8)	-882(4)	6775(2)	7679(2)	32(1)
C(9)	-172(4)	7365(3)	6731(2)	36(1)
C(10)	748(4)	8134(2)	6673(2)	31(1)
C(11)	874(4)	8280(2)	7597(2)	37(1)
C(12)	129(4)	7657(2)	8514(2)	33(1)
C(13)	3811(4)	5593(2)	8551(2)	29(1)
C(14)	4585(4)	6181(2)	7630(2)	30(1)
C(15)	4483(4)	6000(2)	6718(2)	27(1)
C(16)	3601(4)	5200(2)	6794(2)	33(1)
C(17)	2860(4)	4654(2)	7747(2)	30(1)
C(18)	6562(4)	7776(2)	3962(2)	32(1)
C(19)	6321(4)	7737(2)	2990(2)	37(1)
C(20)	7296(5)	8435(3)	2205(2)	41(1)
C(21)	8110(4)	8921(2)	2675(2)	38(1)
C(22)	7667(4)	8531(2)	3764(2)	34(1)
C(23)	5839(4)	7163(2)	4939(2)	33(1)
C(24)	5233(4)	6622(2)	5746(2)	33(1)
Cl(1)	2144(2)	6724(1)	4136(1)	66(1)
Cl(2)	465(2)	5330(1)	3626(1)	70(1)
C(40)	1497(6)	6431(3)	3160(3)	52(1)
Cl(3)	1586(8)	10033(4)	-50(4)	104(2)
C(41)	716(14)	9394(8)	-350(8)	69(3)
Cl(4)	-1214(5)	10133(3)	-350(3)	106(2)

Table 4. Atomic coordinates ($\times 10^4$) and equivalent isotropic displacement parameters ($\text{Å}^2 \times 10^3$) for **11b** U(eq) is defined as one third of the trace of the orthogonalized Uij tensor

Atom	x	y	z	U(eq)
Ag(1)	7453(1)	4595(1)	4945(1)	32(1)
Fe(1)	6204(1)	2371(1)	10340(1)	17(1)
Cl(1)	5973(1)	2801(1)	3193(1)	30(1)
O(1)	5756(3)	3315(1)	3923(1)	52(1)
O(2)	6017(3)	3886(2)	2472(1)	55(1)
O(3)	7723(3)	1999(2)	3210(2)	65(1)
O(4)	4410(3)	2023(2)	3172(1)	53(1)
N(1)	7898(2)	2702(2)	5832(1)	25(1)
N(2)	3067(2)	3504(2)	5912(1)	24(1)
N(3)	656(3)	4063(2)	4047(1)	41(1)
C(1)	8562(2)	2016(2)	9597(1)	21(1)
C(2)	8587(3)	3286(2)	9779(1)	24(1)
C(3)	8584(3)	3093(2)	10656(1)	26(1)
C(4)	8546(3)	1272(2)	11028(1)	26(1)
C(5)	8514(3)	1054(2)	10381(1)	23(1)
C(6)	8528(3)	1781(2)	8784(1)	22(1)
C(7)	8487(3)	1599(2)	8099(1)	23(1)
C(8)	8408(2)	1507(2)	7250(1)	21(1)
C(9)	7996(3)	2665(2)	6641(1)	24(1)
C(10)	8189(3)	1568(2)	5589(1)	26(1)
C(11)	8569(3)	373(2)	6151(1)	27(1)
C(12)	8685(3)	337(2)	6990(1)	25(1)
C(13)	3753(3)	2367(2)	9734(1)	21(1)
C(14)	3839(3)	3582(2)	9973(1)	25(1)
C(15)	3926(3)	3296(2)	10852(1)	27(1)
C(16)	3910(3)	1908(2)	11167(1)	27(1)
C(17)	3822(3)	1325(2)	10482(1)	23(1)
C(18)	3651(3)	2253(2)	8898(1)	23(1)
C(19)	3554(3)	2227(2)	8183(1)	25(1)
C(20)	3421(3)	2230(2)	7322(1)	22(1)
C(21)	3209(3)	3425(2)	6730(1)	23(1)
C(22)	3153(3)	2382(2)	5652(1)	25(1)
C(23)	3384(3)	1157(2)	6200(1)	27(1)
C(24)	3561(3)	1070(2)	7041(1)	26(1)
C(25)	737(3)	4120(2)	3357(1)	33(1)
C(26)	854(3)	4248(2)	2459(1)	52(1)

Table 5. Crystal data, data collection, and structure refinement for compounds **1a**, **1b**, **11a**, **11b**, and **12b**

	1a · 0.5 H ₂ O	1b	11a · 3 CH ₂ Cl ₂	11b · 2 CH ₃ CN	12b
Empirical formula	C ₄₈ H ₃₄ Fe ₂ N ₄ O	C ₂₄ H ₁₆ FeN ₂	C ₅₁ H ₃₈ Fe ₂ N ₄ Ni ₂ O ₁₂	C ₂₆ H ₁₉ AgClFeN ₃ O ₄	
Formula weight	794.49	388.24	1396.72	1273.22	1131.08
Crystal system	Triclinic	Monoclinic	Triclinic	Triclinic	Monoclinic
Space group	<i>P</i> $\bar{1}$	Cc	<i>P</i> $\bar{1}$	<i>P</i> $\bar{1}$	<i>P</i> 2 ₁
<i>a</i> , Å	11.2711(10)	17.261(2)	8.0907(17)	7.0579(8)	6.7738(14)
<i>b</i> , Å	13.3346(12)	9.7914(9)	13.424(2)	10.5149(10)	13.508(3)
<i>c</i> , Å	14.0879(14)	10.8861(16)	13.955(2)	16.5415(15)	24.351(5)
α , deg	105.007(12)	90	71.455(9)	75.829(7)	90
β , deg	105.179(11)	105.366(11)	75.946(11)	85.663(9)	96.73(3)
γ , deg	105.218(10)	90	75.045(14)	85.196(8)	90
<i>V</i> , Å ³	1845.7(3)	1770.8(4)	1366.7	1184.1(2)	2212.7(8)
<i>Z</i>	2	4	1	1	2
<i>d</i> _{calcd.} , g cm ⁻³	1.430	1.456	1.697	1.785	1.698
Temperature, K	298(2)	173(2)	173(2)	173(2)	298(2)
<i>F</i> (000), e	820	800	706	636	1120
Crystal size, mm	0.46×0.22×0.02	0.4×0.4×0.4	0.1×0.4×0.4	0.1×0.8×0.2	0.2×0.5×0.02
Wavelength, Å	0.71073	0.71073	0.71073	0.71073	0.71073
θ limits, deg	2.11 to 24.94	2.41 to 27.49	2.55 to 27.49	2.00 to 27.50	2.94 to 25.92
<i>hkl</i> ranges	-13≤ <i>h</i> ≤13, -15≤ <i>k</i> ≤15, -16≤ <i>l</i> ≤16	-22≤ <i>h</i> ≤22, -12≤ <i>k</i> ≤12, -14≤ <i>l</i> ≤14	-10≤ <i>h</i> ≤8 -16≤ <i>k</i> ≤16 -17≤ <i>l</i> ≤18	-9≤ <i>h</i> ≤9 -13≤ <i>k</i> ≤13 -21≤ <i>l</i> ≤21	-7≤ <i>h</i> ≤7 -16≤ <i>k</i> ≤16 -29≤ <i>l</i> ≤29
Reflections collected	8518	4178	11739	10851	31655
Unique reflections	3535	4054	6214	5426	8266
<i>R</i> (int)	0.0966	0.0284	0.0255	0.0189	0.0879
Completeness to θ = max.	54.7%	100%	99.0%	99.7%	95.0 %
Absorption correction	None	None	Empirical	Empirical	None
Max. and min. transmission			0.3614/0.2643	0.5151/0.3983	
Data/ restraints/ parameters	3535/0/504	4054/ 2 / 453	6214/0/380	5426/ 0 / 327	8266 / 1 / 459
GOF on <i>F</i> ²	0.791	1.955	1.021	1.072	1.372
<i>R</i> 1 ^[a]	0.0640	0.0317	0.0425	0.0236	0.1324
<i>wR</i> 2 ^[b]	0.1292	0.0891	0.1115	0.0613	0.3765
Extinction coefficient		0.0106(13)	0.0024	0.0082(4)	0.0000(16)
Largest diff. peak and hole, e Å ³	0.980/-0.373	0.120/-0.252	1.175/-0.696	0.520/-0.500	2.823 and -2.497

$$^{[a]} R1 = \frac{\sum ||F_o| - |F_c||}{\sum |F_o|}, \quad ^{[b]} wR2 = \left[\frac{\sum [w(F_o^2 - F_c^2)^2]}{\sum [w(F_o^2)^2]} \right]^{0.5}.$$

4 References

- ¹ J. Moutet, E. Saint-Aman, G. Royal, S. Tingry, R. Ziessel, *Eur. J. Inorg. Chem.* **2002**, 692-698.
- ² A. Ion, J. Moutet, E. Saint-Aman, G. Royal, S. Tingry, J. Pecaut, S. Menage, R. Ziessel, *Inorg. Chem.* **2001**, *40*, 3632-3636.
- ³ M. Buda, J. Moutet, E. Saint-Aman, A. De Cian, J. Fischer, R. Ziessel, *Inorg. Chem.* **1998**, *37*, 4146-4148.
- ⁴ N. Sachsinger, C. D. Hall, *J. Organomet. Chem.* **1997**, *531*, 61-65.
- ⁵ C. D. Hall, T. Truong, S. C. Nyburg, *J. Organomet. Chem.* **1997**, *547*, 281-286.
- ⁶ B. König, M. Nimtz, H. Zieg, *Tetrahedron* **1995**, *51*, 6267-6272.
- ⁷ I. R. Butler, *Organometallics* **1992**, *11*, 74-83.
- ⁸ I. R. Butler, J. L. Rouston, *Can. J. Chem.* **1990**, *68*, 2212-2215.
- ⁹ E. Sondaz, J. Jaud, J. -P. Launay, J. Bonvoisin, *Eur. J. Inorg. Chem.* **2002**, 1924-1927.
- ¹⁰ D. Astruc, *Acc. Chem. Res.* **1997**, *30*, 383-391.
- ¹¹ J. -P. Launay, *Chem. Soc. Rev.* **2001**, *30*, 386-397.
- ¹² E. C. Constable, A. J. Edwards, R. Martinet-manez, P. R. Raithby, A. M. W. Thompson, J. *Chem. Soc. Dalton Trans.* **1994**, 645-650.
- ¹³ J. D. Carr, S. J. Coles, M. B. Hursthouse, M. E. Light, E. L. Munro, J. H. R. Tucker, J. Westwood, *Organometallics* **2000**, *19*, 3312-3315.
- ¹⁴ J. Alvarez, A. E. Kaifer, *Organometallics* **1999**, *18*, 5733-5734.
- ¹⁵ Y. Wang, S. Mendoza, A. E. Kaifer, *Inorg. Chem.* **1998**, *37*, 317-320.
- ¹⁶ K. R. Justin Thomas, J. T. Lin, Y. S. Wen, *Organometallics* **2000**, *19*, 1008-1012.
- ¹⁷ O. Lavastre, J. Plass, P. Bachmann, S. Guesmi, C. Moinet, P. H. Dixneuf, *Organometallics* **1997**, *16*, 184-189.
- ¹⁸ D. Osella, L. Milone, C. Nervi, M. Ravera, *J. Organomet. Chem.* **1995**, *488*, 1-7.
- ¹⁹ D. Astruc, M. Lacoste, L. Toupet, *J. Chem. Soc. Chem. Commun.* **1990**, 558-561.

- ²⁰ J. V. Ortega, B. Hong, S. Ghosal, J. C. Hemminger, B. Breedlove, C. P. Kubiak, *Inorg. Chem.* **1995**, *38*, 5102-5112.
- ²¹ J. P. Strachan, S. Gentemann, J. Seth, W. A. Kalsbeck, J. S. Lindsey, Dewey Holten, D. F. Bocian, *J. Am. Chem. Soc.* **1997**, *119*, 11191-11201.
- ²² F. Barriere, N. Camire, W. E. Geiger, U. T. Mueller-Westerhoff, R. Sanders, *J. Am. Chem. Soc.* **2002**, *124*, 7262-7263.
- ²³ M. Brady, W. Q. Weng, J. A. Gladysz, *J. Chem. Soc., Chem. Commun.* **1994**, 2655-2656.
- ²⁴ J. Seth, V. Palaniappan, R. W. Wagner, T. E. Johnson, J. S. Lindsey, D. F. Bocian, *J. Am. Chem. Soc.* **1996**, *118*, 11194-11207.
- ²⁵ S. Barlow, D. O'Hare, *Chem. Rev.* **1997**, *97*, 637-669.
- ²⁶ S. Leininger, B. Olenyuk, P. J. Stang, *Chem. Rev.* **2000**, *100*, 853-908.
- ²⁷ M. Fujita, *Chem. Soc. Rev.* **1998**, *27*, 417-425.
- ²⁸ B. Olenyuk, A. Fechtenkötter, P. J. Stang, *J. Chem. Soc., Dalton Trans.* **1998**, 1707-1728.
- ²⁹ F. A. Cotton, C. Lin, C. A. Murillo, *Inorg. Chem.* **2001**, *40*, 478-484.
- ³⁰ F. A. Cotton, L. M. Daniels, C. Lin, C. A. Murillo, *J. Am. Chem. Soc.* **1999**, *121*, 4538-4539.
- ³¹ P. J. Stang, B. Olenyuk, J. Fan, A. M. Arif, *Organometallics* **1996**, *15*, 904-908.
- ³² M. Pilkington, S. Decurtins, *Chimia* **2001**, *55*, 1014-1016.
- ³³ J. C. Noveron, M. S. Lah, R. E. Del Sesto, A. M. Arif, J. S. Miller, P. J. Stang, *J. Am. Chem. Soc.* **2002**, *124*, 6613-6625.
- ³⁴ A. Rodriguez-Fortea, P. Alemany, S. Alvarez, E. Ruiz, A. Sculler, C. Decroix, V. Marvaud, J. Vaissermann, M. Verdager, I. Rosenman, M. Julve, *Inorg. Chem.* **2001**, *40*, 5868-5877.
- ³⁵ M. Conrad, F. Meyer, A. Jacobi, P. Kircher, P. Rutsch, L. Zsolnai, *Inorg. Chem.* **1999**, *38*, 4559-4566.
- ³⁶ D. Volkmer, A. Hörstmann, K. Griesar, W. Haase, B. Krebs, *Inorg. Chem.* **1996**, *35*, 1132-1135.
- ³⁷ E. Lindner, R. F. Zong, K. Eichele, *Phosphorus, Sulfur and Silicon* **2001**, *169*, 219-222.
- ³⁸ E. Lindner, R. F. Zong, K. Eichele, M. Ströbele, *J. Organomet. Chem.* **2002**, *660(1)*, 78-84.
- ³⁹ C. J. Kuehl, S. D. Huang, P. J. Stang, *J. Am. Chem. Soc.* **2001**, *123*, 9634-9641.

- ⁴⁰ A. Khatyr, R. Ziessel, *J. Org. Chem.* **2000**, *65*, 7814-7824.
- ⁴¹ P. F. H. Schwab, F. Fleischer, J. Michl, *J. Org. Chem.* **2002**, *67*, 443-449.
- ⁴² D. Tzalis, Y. Tor, S. Failla, J. S. Siegel, *Tetrahedron Lett.* **1995**, *36*, 3489-3490.
- ⁴³ J. Polin, E. Schmohel, V. Balzani, *Synthesis* **1998**, *3*, 321-324.
- ⁴⁴ M. Schmittel, C. Michel, A. Wiegrefe, V. Kalsani, *Synthesis* **2001**, *10*, 1561-1567.
- ⁴⁵ P. J. Connors, D. Jr. Tzalis, A. L. Dunnick, Y. Tor, *Inorg. Chem.* **1998**, *37*, 1121-1123.
- ⁴⁶ K. Sonogashira, Y. Tohda, N. Hagihara, *Tetrahedron Lett.* **1975**, *50*, 4467-4470.
- ⁴⁷ R. F. Kovar, M.D. Rausch, H. Rosenberg, *Organometal. Chem. Syn.* **1970/1971**, *1*, 173-181.
- ⁴⁸ R. Ziessel, J. Suffert, M. -T. Youinou, *J. Org. Chem.* **1996**, *61*, 6535-6546.
- ⁴⁹ V. Grosshenny, F. M. Romero, R. Ziessel, *J. Org. Chem.* **1997**, *62*, 1491-1500.
- ⁵⁰ O. Lavastre, M. Even, P. H. Dixneuf, *Organometallics* **1996**, *15*, 1530-1531.
- ⁵¹ S. Höger, K. Bonrad, A. Mourran, U. Beginn, M. Möller, *J. Am. Chem. Soc.* **2001**, *123*, 5651-5659.
- ⁵² C. J. Yu, Y. Ch. Chong, J. F. Kayyem, M. Gozin, *J. Org. Chem.* **1999**, *64*, 2070-2079.
- ⁵³ T. M. Swager, C. J. Gil, M. S. Wrighton, *J. Phys. Chem.* **1995**, *99*, 4886-4893.
- ⁵⁴ H. Meier, H. Aust, *J. Prakt. Chem.* **1999**, *341*, 466-471.
- ⁵⁵ S. Höger, K. Bonrad, G. Schäfer, V. Z. Enkelmann, *Z. Naturforsch.* **1998**, *53b*, 960-964.
- ⁵⁶ Z. N. Bao, Y. M. Chen, R. B. Cai, L. P. Yu, *Macromolecules* **1993**, *26*, 5281-5286.
- ⁵⁷ F. Gelin, R. P. Thummel, *J. Org. Chem.* **1992**, *57*, 3780-3783.
- ⁵⁸ U. Siemeling, U. Vorfeld, B. Neumann, H. -G. Stammler, *Chem. Ber.* **1995**, *128*, 481-485.
- ⁵⁹ E. Lindner, R. F. Zong, K. Eichele, U. Weisser, M. Ströbele, *Eur. J. Inorg. Chem.* submitted.
- ⁶⁰ P. Knops, N. Sendhoff, H. -B. Meikelburger, F. Vögtle, *High Dilution Reactions - New Synthetic Applications: Topics in Current Chemistry* (Eds. E. Weber, F. Vögtle), Springer, Heidelberg, **1992**.
- ⁶¹ A. N. Khlobystov, A. J. Blake, N. R. Champness, D. A. Lemenovskii, A. G. Majouga, N. V. Zyk, M. Schröder, *Coord. Chem. Rev.* **2001**, *222*, 155-192.

- ⁶² W. M. Xue, F. E. Kühn, E. Herdtweck, Q.C. Li, *Eur. J. Inorg. Chem.* **2001**, 213-221.
- ⁶³ Y. Uchida, R. Kajita, Y. Kasasaki, S. Oae, *Tetrahedron Lett.* **1995**, *36*, 4077-4080.
- ⁶⁴ K. Kurtev, D. Ribola, R. A. Jones, D. J. Cole-Hamilton, G. Wilkinson, *J. Chem. Soc., Dalton Trans.* **1980**, 55-58.
- ⁶⁵ D. Drew, J. R. Doyle, *Inorg. Synth.* **1990**, *28*, 346-349.
- ⁶⁶ P. Four and F. Guibe, *J. Org. Chem.* **1981**, *46*, 4439-4445.
- ⁶⁷ O. Dangles, F. Guibd, G. Balavoine, S. Lavielle and A. Marquet, *J. Org. Chem.* **1987**, *52*, 4984-4993.
- ⁶⁸ m: low field part of an AA'XX' pattern, $N = |^3J_{\text{HH}} + ^5J_{\text{HH}}|$
- ⁶⁹ m: high field part of an AA'XX' pattern, $N = |^3J_{\text{HH}} + ^5J_{\text{HH}}|$
- ⁷⁰ V. Jullien, M. W. Hosseini, J. -M. Planeix, A. D. Cian, *J. Organomet. Chem.* **2002**, *634-644*, 376-380.
- ⁷¹ G. M. Sheldrick, *SHELXTL V5.03, Program for crystal structure refinement*, University of Göttingen, Germany **1995**.
- ⁷² G. M. Sheldrick, *Acta Crystallogr. Sect. A* **1995**, *51*, 33-38. ("SHELXS V5.03 program for crystal structure solution", University of Göttingen, Germany).
- ⁷³ G. M. Sherdrick, *SHELXTL V5.03*, University of Göttingen, Germany, **1995**.
- ⁷⁴ S. Dümmling, E. Eichhorn, S. Schneider, B. Speiser, M. Würde, *Curr. Sep.* **1996**, *15*, 53-56.

5 Summary

Electronic communication between linked metal centers has been an attractive subject of many studies. Electronic interaction could lead to a new series of electrochemical sensors for detection and quantitative analysis of metals. As a consequence of oxidizing or reducing one of the metals, complexation/decomplexation, or the reactivity of the other metal linked to the first one could be modulated. Long distance through bond electronic interaction between metals connected by nanometer-sized, conjugated bridges is gaining attention in material science. In this context, the synthesis of conjugated rigid ligand systems which are able to function as valuable precursors for the access to macrocycles with the potential to show electronic communication is of interest. Building blocks for the construction of these ligands are 1,1'-ferrocenediyl, pyridine-4-yl, pyridine-3-yl, 2,2'-bipyridine-5-yl, and 1,10-phenanthroline-3-yl, acetylene or nanometer-sized 1,4-diethynylbenzene. These positions are preferred based on geometrical and electronic considerations. The objective of this work is the construction of such ligands and their metallamacrocyclic complexes as well as the investigation of electronic interactions between the linked metals by means of cyclic voltammetry.

In the first part of this thesis, the synthesis and characterization of bidentate and tetradentate ligands of the type $[\eta^5\text{-C}_5\text{H}_4\text{-C}_2\text{-R}]_2\text{Fe}$ (R = pyridine-4-yl, pyridine-3-yl, and 2,2'-bipyridine-5-yl) and $[\eta^5\text{-C}_5\text{H}_4\text{-C}_2\text{-C}_6\text{H}_2(\text{OR}')_2\text{-C}_2\text{-R}]_2\text{Fe}$ (R = pyridine-4-yl, pyridine-3-yl, 2,2'-bipyridine-5-yl, 1,10-phenanthroline-3-yl and R' = *n*-C₃H₇) are described. Ligands $[\eta^5\text{-C}_5\text{H}_4\text{-C}_2\text{-R}]_2\text{Fe}$ were accessible by Sonogashira C-C coupling reactions of 1,1'-diiodoferrocene with 4-/3-ethynylpyridine and 5-ethynyl-2,2'-bipyridine, which were obtained by using modified literature methods. They represent red solids with melting points higher than 185°C. Two molecules of 1,1'-bis(4-pyridylethynyl)ferrocene and one water molecule crystallizes in the triclinic space group $P\bar{1}$ with $Z = 2$. Both 4-pyridylethynylcyclopentadienyl units are nearly parallel (eclipsed), generating a *syn*-conformer of the ferrocene. The water molecule is hydrogen-bonded to the N-atoms of the

pyridines. In contrast to that of its isomer, 1,1'-bis(3-pyridylethynyl)ferrocene crystallizes in the monoclinic space group Cc with $Z = 4$. Disorder of the molecules in the crystals is established. Both 3-pyridylethynylcyclopentadienyl groups are also almost parallel (eclipsed), creating a *syn*-conformer of this ferrocene.

On the other hand, the preparation of *N*-functionalized ligands $[\eta^5\text{-C}_5\text{H}_4\text{-C}_2\text{-C}_6\text{H}_2(\text{OR}')_2\text{-C}_2\text{-R}]_2\text{Fe}$ was carried out by different methods which are characterized by pre-organization of a key precursor, like $[\eta^5\text{-C}_5\text{H}_4\text{-C}_2\text{-C}_6\text{H}_2(\text{OR}')_2\text{-C}_2\text{-R}]_2\text{Fe}$ ($R = \text{triisopropylsilyl}$). Palladium-catalyzed coupling reaction of 1,1'-diiodoferrocene and 1-ethynyl-4-(triisopropylsilylethynyl)-2,5-dipropoxybenzene readily afforded the desired compound. The latter was obtained by multi-step organic syntheses, Williamson ether synthesis from hydroquinone and *n*-iodopropane, mono-bromination with bromine and mono-iodination with I_2/HIO_3 of the ether, followed by selective palladium-mediated C-C coupling with triisopropylsilylacetylene and trimethylsilylacetylene, and finally cleavage of the trimethylsilyl group in the presence of NaOH in methanol. An one-pot, two-step reaction furnished the conversion of R from triisopropylsilyl to pyridine-4-yl, pyridine-3-yl, 2,2'-bipyridine-5-yl, and 1,10-phenanthroline-3-yl. First, the triisopropylsilyl groups were removed by tetra-*n*-butylammonium fluoride in THF. Then, a Sonogashira coupling reaction of the deprotected 1,1'-ferrocenedi(ethynyl) intermediate with bromo-derivatives of the corresponding aromatic N-heterocycles afforded the target ligands. These ferrocenes were obtained as red, air stable solids, which are soluble in common organic solvents. All these novel ligands are characterized spectroscopically and by elemental analysis.

The tetranuclear macrocyclic complexes $[(\eta^5\text{-C}_5\text{H}_4\text{-C}_2\text{-4-C}_5\text{H}_4\text{N})_2\text{Fe}]_2\text{Ni}_2(\text{NO}_3)_4$, $[(\eta^5\text{-C}_5\text{H}_4\text{-C}_2\text{-3-C}_5\text{H}_4\text{N})_2\text{Fe}]_2\text{Ag}_2(\text{ClO}_4)_2$, and $[(\eta^5\text{-C}_5\text{H}_4\text{-C}_2\text{-3-C}_5\text{H}_4\text{N})_2\text{Fe}]_2\text{Pd}_2\text{Cl}_4$ were obtained by reaction of $[\text{Ni}(\text{H}_2\text{O})_6](\text{NO}_3)_2$, AgClO_4 , and $\text{PdCl}_2(\text{COD})$ with the ligands $(\eta^5\text{-C}_5\text{H}_4\text{-C}_2\text{-4-C}_5\text{H}_4\text{N})_2\text{Fe}$ and $(\eta^5\text{-C}_5\text{H}_4\text{-C}_2\text{-3-C}_5\text{H}_4\text{N})_2\text{Fe}$, respectively, under high dilution conditions. Both compounds $[(\eta^5\text{-C}_5\text{H}_4\text{-C}_2\text{-4-C}_5\text{H}_4\text{N})_2\text{Fe}]_2\text{Ni}_2(\text{NO}_3)_4 \cdot 3 \text{CH}_2\text{Cl}_2$ and $[(\eta^5\text{-C}_5\text{H}_4\text{-C}_2\text{-3-C}_5\text{H}_4\text{N})_2\text{Fe}]_2\text{Ag}_2(\text{ClO}_4)_2 \cdot 2 \text{CH}_3\text{CN}$ crystallize in the triclinic space group $P\bar{1}$ and each molecule

has a center of symmetry, while the palladium complex crystallizes in the space group $P2_1$. Further characterization succeeded by elemental analyses, ^1H NMR, and IR spectra. Molecule $[(\eta^5\text{-C}_5\text{H}_4\text{-C}_2\text{-4-C}_5\text{H}_4\text{N})_2\text{Fe}]_2\text{Ni}_2(\text{NO}_3)_4$ represents an unsymmetric paddlewheel, in which the centers of the four Cp rings define a nearly ideal rectangle with a dimension of 20.2×3.3 Å. The metal-metal distances are 20.2 (Fe-Fe), 3.39 (Ni-Ni), and 10.2 (Fe-Ni) Å. The nitrates are coordinated in two different modes to the nickel centers. Two of them function as μ_2 -bridging ligands, whereas the other two are η^2 -chelated. The included dichloromethane molecules are head-to-head arranged and hydrogen-bonded in two different ways to the nitrates. In principle macrocycles $[(\eta^5\text{-C}_5\text{H}_4\text{-C}_2\text{-3-C}_5\text{H}_4\text{N})_2\text{Fe}]_2\text{Ag}_2(\text{ClO}_4)_2$ and $[(\eta^5\text{-C}_5\text{H}_4\text{-C}_2\text{-3-C}_5\text{H}_4\text{N})_2\text{Fe}]_2\text{Pd}_2\text{Cl}_4$ can also be described as rectangles, however, due to the 3-positioned nitrogen donors with deformed edges. In the silver complex, the perchlorates are *pseudo*-bridging the two silver(I) atoms. The molecular structure of the palladium(II) complex $[(\eta^5\text{-C}_5\text{H}_4\text{-C}_2\text{-3-C}_5\text{H}_4\text{N})_2\text{Fe}]_2\text{Pd}_2\text{Cl}_4$ is similar to that of silver(I), but each palladium atom is additionally coordinated to two *trans*-positioned chlorides with an arrangement of PdCl_2 units about 45° to the pyridine rings. Intramolecular metals are separated by 17.34 (Fe-Fe), 3.50 (Ag-Ag), and 8.65/9.03 (Fe-Ag) for the former and 17.61 (Fe-Fe), 4.12 (Pd-Pd), and 8.94/9.13 Å (Fe-Pd) for the latter. In contrast to the offset packing of the dinickel molecules, the disilver molecules in the crystal are aligned by acetonitrile bridges, forming a supramolecular network with intra- and intermolecular Ag-Ag distances of 3.50 and 3.79 Å, respectively.

The rich coordination chemistry of the bis(bidentate) ligands $[\eta^5\text{-C}_5\text{H}_4\text{-C}_2\text{-C}_6\text{H}_2(\text{OR}')_2\text{-C}_2\text{-R}]_2\text{Fe}$ (R = 2,2'-bipyridine-5-yl, 1,10-phenanthroline-3-yl) was demonstrated by the readily formation of bimetallic complexes $[\eta^5\text{-C}_5\text{H}_4\text{-C}_2\text{-C}_6\text{H}_2(\text{OR}')_2\text{-C}_2\text{-R}]_2\text{FeM}$ (R = bipy, M = Zn^{2+} ; R = phen, M = Ag^+ , Zn^{2+} , Fe^{2+}) at room temperature. No electronic interaction between the linked metals has been established, which is ascribed to the long distance of more than 13 bonds between the metal atoms and the relative rigidity of the molecules.

Cyclovoltammetric studies revealed chemically reversible ferrocene-based redox reactions of 1,1'-bis(4-/3-pyridylethynyl)ferrocene and the dinickel as well as the disilver complex. No long-distance through bond electronic communication between the two identical ferrocene units was established in the macrocyclic complexes. Mainly two factors should be responsible for this observation. Both ferrocene building blocks are separated by a distance of more than 1.7 nm, thus too far away to communicate. Moreover the Ni₂ and Ag₂ cores fail to transmit the η^5 -C₅H₄-C₂-C₅H₄N conjugation. However, a weak influence of the Ni(II) and Ag(I) atoms through the conjugated bonds on the redox potential of the ferrocene units has been established in spite of a distance of 1 nm. In the nickel(II) complex a weak antiferromagnetic interaction between the intramolecularly arranged nickel(II) atoms was found.

Meine akademische Ausbildung verdanke ich:

– H. J. Cao – L. Y. Qu – E. Lindner – H. Z. Liang – J. F. Liu – T. Z. Nie – H. F. Sheng – B.

Speiser – J. Strähle – Y. C. Su – J. G. Wu – Z. H. Xu – K.-P. Zeller – B. L. Zhao – C. D. Zhao

– S. L. Zhao – E. B. Wang – Z. P. Wang – S. F. Weng.

Lebenslauf

Persönliche Daten

Name Ruifa Zong (宗瑞发)
Geburtstag/-ort: 26. September 1962 in ShanDong
Eltern: Jinghe Zong
Fengrong Zhang
Staatsangehörigkeit: Volksrepublik China

Schulbildung

Sept. 1970 - Juli 1975 Grundschule in Fuxing
Sept. 1975 - Juli 1978 Gymnasium in Fuxing
Sept. 1978 - Juli 1980 Nr. 1 -Gymnasium in Helong

Hochschulbildung

09. 1980 - 07. 1984 Chemiestudium an der Nordost-Lehrausbildungs-Universität in ChangChun
07. 07. 1984 Zeugnis des Bachelor Degree of Science
09. 1984 - 07. 1987 Graduiertenstudium unter der Leitung von Herrn Prof. J. F. Liu, Herrn Prof. Sh. L. Zhao und E. B. Wang am Institut für Anorganische Chemie der Nordost-Lehrausbildungs-Universität mit dem Thema “ Synthese und Charakterisierung von Lanthaniden Komplexen mit 11-Tungstometallat-Liganden”
01. 07. 1987 Zeugnis des Master Degree of Science
01. 1999 - 10. 2002 Dissertation unter Leitung von Herrn Prof. Dr. E. Lindner am Institut für Anorganische Chemie der Universität Tübingen mit dem Titel “ Selbstorganisierte molekulare Polygone aus konjugierten 1,1'-Ferrocendiyl-verbrückten Bis(pyridinen), Bis(2,2'-bipyridinen) und Bis(1,10-phenanthrolinen) und Übergangsmetallen als Bausteine ”

Beschäftigung

07. 1987 - 12. 1998 Assistent, Priv. -Doz. und Professor für Chemie an der Hauptstadt-Lehrausbildungs-Universität in Peking
09. 1996 - 07. 1997 Gastwissenschaftler unter der Leitung von Frau Prof. J. G. Wu an der Peking-Universität mit dem Thema “ Synthese und spektroskopische Charakterisierung von Lanthaniden-Zucker-Komplexen”
06. 1999 - 10. 2002 Wissenschaftlicher Angestellter der Universität Tübingen im Anorganisch-Quantitativen Praktikum am Institut für Anorganische Chemie der Universität Tübingen